MARCH 2018 M.Sc. In Electrical & Electronic Engineering AMER HASAN MAHMOOD AL-SHATHR

UNIVERSITY OF GAZIANTEP
GRADUATE SCHOOL OF
NATURAL & APPLIED SCIENCES

MINIATURIZATION OF MICROSTRIP ANTENNAS USING METAMATERIALS

M.Sc. THESIS

IN

ELECTRICAL AND ELECTRONIC ENGINEERING

BY

AMER HASAN MAHMOOD AL-SHATHR

MARCH 2018

Miniaturization of Microstrip Antennas Using Metamaterials

M.Sc. Thesis

in

Electrical & Electronic Engineering

University of Gaziantep

Supervisor

Assoc. Prof. Dr. Gölge ÖGÜCÜ YETKİN

By

Amer Hasan Mahmood AL-SHATHR

March 2018

REPUBLIC OF TURKEY
UNIVERSITY OF GAZIANTEP
GRADUATE SCHOOL OF NATURAL & APPLIED SCIENCES
ELECTRICAL AND ELECTRONICS ENGINEERING

Name of the thesis: Miniaturization of Microstrip Antennas using Metamaterials

Name of the student: Amer Hasan Mahmood AL-SHATHR

Exam date: 02.03.2018

Approval of the Graduate School of Natural and Applied Sciences

Prof. Dr. Ahmet Necmeddin YAZICI
Director

I certify that this thesis satisfies all the requirements as a thesis for the degree of Master of Science.

Prof. Dr. Ergun ERÇELEBİ
Head of Department

This is to certify that we have read this thesis and that in our consensus opinion; it is fully adequate, in scope and quality, as a thesis for the degree of Master of Science.

Assoc. Prof. Dr. Gölge ÖGÜCÜ YETKİN
Supervisor

Examining Committee Members:	Signature
Prof. Dr. Savaş UÇKUN	.....
Assoc. Prof. Dr. Gölge ÖGÜCÜ YETKİN	.....
Assoc. Prof. Dr. Muharrem KARAASLAN	.....

I hereby declare that all information in this document has been obtained and presented in accordance with academic rules and ethical conduct. I also declare that, as required by these rules and conduct, I have fully cited and referenced all material and results that are not original to this work.

Amer Hasan Mahmood AL-SHATHR

ABSTRACT

MINIATURIZATION OF MICROSTRIP ANTENNAS USING METAMATERIALS

AL-SHATHR, Amer Hasan Mahmood
M.Sc. in Electrical & Electronic Engineering
Supervisor: Assoc. Prof. Dr. Gölge ÖGÜCÜ YETKİN
March 2018, 77 Pages

This research focuses on several main goals, including the design of a multiband rectangular microstrip patch antenna with spacious bandwidth and high return loss by using Complementary Split Ring Resonator (CSRR) beside the Rectangular Ruler Patches (RRPs), improvement the performance of Wi-MAX and GPS applications by using Circular Head Dumbbell Structure (CHDS) beside Circular Ring Patches (CRPs), study the behavior of CHDS on three types of conventional antennas as a redirector, miniaturization the size of the microstrip patch by using (CSRR), (CHDS), (RRPs), (CRPs) and Circular patch (CP). A patch antenna is designed and simulated for 4.66 and 5.61 GHz. Two substrates of FR-4 lossy are utilized with 4.3 dielectric constant, 1.4mm and 0.2mm thickness. The shape is used for conventional patch antenna as rectangular with a central feed source. The RISs have been used as secondary or additional patches with CSRR and as main patches with CHDS, which behaves as a redirector. The conventional antenna operates at a frequency band of 4.66 GHz and 5.61 GHz, while the designed antenna with CSRR and RRPs generates four wide band resonant modes at 4.36, 4.7, 5.6 and 5.9 GHz, therefore It is considered as a multi-use antenna. The designed antenna with CHDS and CRPs generates two band resonant modes at 1.55 GHz and 5.68 GHz.

Keywords: Complementary Split Ring Resonator CSRR, Rectangular Ruler Patches RRPs,WiMAX, GPS, Circular Head Dumbbell Structure CHDS, Circular Ring patch CRPs.

ÖZET

METAMATERYALLER KULLANILARAK MİKROŞERİT ANTENLERİN MİNYATÜRİZE EDİLMESİ

AL-SHATHR, Amer Hasan Mahmood
Yüksek Lisans Tezi/ Elektrik & Elektronik Mühendisliği
Danışman: Doç. Dr. Gölge ÖGÜCÜ YETKİN
Mart 2018, 77 sayfa

Bu araştırma, Dikdörtgen Ruler Yamalarının (RRP'ler) yanında Tamamlayıcı Split Halka Rezonatör (CSRR) kullanarak, Wi-MAX'ın performansını geliştirerek, geniş bant genişliği ve yüksek geri dönüş kaybına sahip çok bantlı dikdörtgen mikro şerit yama anteninin tasarımı da dahil olmak üzere, birkaç ana hedef üzerine odaklanmaktadır ve GPS uygulamalarında, Dairesel Halka Yamalar (CRDS) yanında Yuvarlak Başlı Dambıl Yapısı (CHDS) kullanarak, üç tip geleneksel anten üzerinde bir yeniden yönlendirici olarak CHDS'nin davranışını incelemek, (CSRR), (CHDS) kullanarak mikro band hattının boyutunu minyatürize etmek,), (RRPs), (CRPs) ve dairesel yama (CP). Bir yama anteni 4.66 ve 5.61 GHz için tasarlanmış ve simüle edilmiştir. FR-4 kayıplı iki substrat, 4.3 dielektrik sabiti, 1.4 mm ve 0.2 mm kalınlıkta kullanılır. Şekil, konvansiyonel yama anteni için merkezi bir besleme kaynağı olan dikdörtgen olarak kullanılır. RIS'ler, CSRR ile birlikte ikincil veya ek yamalar olarak ve yeniden yönlendirme görevini gören CHDS ile ana yamalar olarak kullanılmıştır. CSRR ve RRP'li tasarlanmış anten 4.36, 4.7, 5.6 ve 5.9 GHz'de dört geniş bant rezonant modu üretirken geleneksel anten 4.66 GHz ve 5.61 GHz frekans bandında çalışır; bu nedenle çoklu kullanımlı bir anten olarak kabul edilir. CHDS ve CRP'lere sahip tasarlanmış anten, 1.55 GHz ve 5.68 GHz'de iki bant rezonant modu üretir.

Anahtar Kelimeler: Tamamlayıcı Split Halka Rezonatör CSRR, Dikdörtgen Cetvel Yamalar RRPs, WiMAX, GPS, Dairesel Başlı Dambıl Yapı CHDS, Dairesel Halka Yamalar CRPs.

To My

Dear **father** and **mother** who encouraged and supported me throughout my life, my **brothers**, **friends** and everyone stood beside me

ACKNOWLEDGEMENT

First and foremost, thanks to **Allah**, the creator of the universes and the only one we resort to in times of adversity.

I would like to thank my respected supervisor **Assoc. Prof. Dr. Gölge ÖGÜCÜ YETKİN**, Department of Electrical & Electronic Engineering, University of Gaziantep, Gaziantep-Turkey. The door to **Assoc. Prof. Dr. YETKİN** office was always open whenever I ran into a trouble spot or had a question about my research or writing. She steered me in the right the direction whenever she thought I needed it.

Finally, I must express my very profound gratitude to my **Parents** for providing me with unfailing support and continuous encouragement throughout my years of study and through the process of researching and writing this thesis. This accomplishment would not have been possible without them. Thank you.

TABLE OF CONTENTS

LIST OF FIGURES

Page

LIST OF TABLES

Page

LIST OF SYMBOLS/ ABBREVIATIONS

BWM	Backward Wave Materials
CSRR	Complementary Split Ring Resonator
CHDS	Circular Head Dumbbell Structure
CRPs	Circular Ring Patches
CP	Circular Patch
CST	Computer Simulation Technology
C	Speed of light
DGS	Defected Ground Structure
Ea	Electric Field
ε_reff	Effective Permittivity
ε_r	Relative Permittivity
ε	Permittivity or Dielectric constant
GPS	Global Positioning System
GSM	Global System for Mobile communication
GHz	Giga Hertz
Ha	Magnetic Field
Jt	Current Density of top patch surface
Jb	Current Density of bottom patch surface
Js	Current Density
L1	Length of substrate
L2	Length of patch
LHM	Left-Handed Materials
λ	Wave Length
MPA, MSPA	Microstrip Patch Antenna
MHz	Mega Hertz
Ms	Magnetic Current Density

Pi	Input Power
Pr	Reflected Power
PP	Polar Plot
μ	Permeability
μ_eff	Effective Permeability
RRPs	Rectangular Ruler Patches
RIS	Reactive Impedance Surface
RFID	Radio Frequency Identification
RP	Radiation Pattern
Γ	Rate of reflected wave to the fallen wave
RF	Radio Frequency
SRR	Split Ring Resonator
TE	Transverse Electric
TM	Transverse Magnetic
TEM	Transverse Electric and Magnetic
T1 , T2	Thickness of substrate
T3	Thickness of patch
t	Thickness of ground
Wi-MAX	Worldwide Interoperability for Microwave Access
WLAN	Wireless Local Area Network
W1	Width of substrate
W2	Width of patch

CHAPTER 1

INTRODUCTION

1.1 General

It has become axiomatic and known to most of the searchers in the world of wireless communications that Microstrip patch antenna has a priority in many uses because of the unique features that make it a target for developers such simple in manufacturing, tiny size, lower cost than others, lightweight, has the ability to integrate with integrated microwave circuits and identically with the curved surface [1]. The first microstrip patch antenna was formed as early as 1970[2]. The first proposal to design a microstrip antenna was by Deschamps in 1953, where gained considerable attention later [3]. There are certain techniques used to feed the microstrip patch antenna, each technique has its own special handling with the application type [4], like microstrip line feed, probe feed, proximity feed and aperture feed. Also, by changing the structural form or the type of fabricated material which lead to a change in physical behavior, many results can be obtained in terms of pattern, concentration of energy, polarization, impedance and diversity of resonant frequencies. All that was features of this type of antennas, the disadvantages encountered by developers or researchers, which are considered from characteristics of this antenna, are narrow bandwidth and weakly polarization pureness [5]. However, the researchers have taken many strategies to overcome these constraints and inhance the bandwidth, which is the antenna workspace at a given frequency.

1.1.1 Modes of MPA Analyzing

There are several reasons for the importance of antenna analysis [6]:

- It can be exploited for properties of nearby fields like antenna efficiency, impedance bandwidth, input impedance and mutual coupling also foretells the radiance features such as the gain, radiation pattern and polarization.
- Realize the characteristics and determinations of the antenna through parameters performance study.

- For adjustments to a present design and for the development of renewed antenna formations as well as understanding operation fundamentals that may be helpful for a new design [6].

1.1.2 Miniaturization of Microstrip Patch

Minimizing the size of patch antenna has become highly required from wireless communications. From that standpoint, small size patches with similar performance or better than the large size have been required. In case of lower frequencies, the microstrip patch size need to be large for controllable. There are several technicalities used to minimize the size of patch antenna, like:

- Design dielectric substrate has a high permittivity [7].
- Placement of reactive or resistive load [8].
- Enhancing the antenna form in order to increase the electrical length [9].
- Design a structure with embedded slots on the patch [10].

1.1.2.1 Previous Research Studies Conducted by Researchers on minimization

- V. Rajesh Kumar et al. (2013) presented a MPA with double band properties and CSRR structure which employed in the ground plane. It was observed during the simulation results obtained that the size of the antenna can be reduced with the dual band operation. The radiant patch compared with the conventional MPA has a reduction in size of 89%. Also, the changing in resonance frequency with the change in CSRR length was analyzed [11].
- In the work of (2013) by I. B. Issa et al, a multiband compact antenna with square shape of CSRR was presented. The suggested antenna can be inserted seamlessly with RF front-end circuits used in mobile handsets due to its small size. The wireless communication standards and diverse frequency bands can be efficiently covered by the antenna which includes, (Wi-Fi) 2.4GHz, (Wi-Max) 3.5GHz, (UWB) 7.8-9.1GHz, and (10.9-11.5) GHz, (17.2-17.8) GHz frequency bands. Furthermore, the antenna gain values made it suitable for both outdoor and indoor wireless communications [12].
- M. M. Bait-Suwailam et al. (2013) proposed unfamiliar design of MPA with a slotted CSRR structure in order to miniaturize the size of antenna and called

by SCSRR. The size of MPA decreased by 10% with employment of SCSRR in ground plane as well as mutual coupling between MPAs. The results simulated by CST Microwave Studio [13].

- In the work of (2013) by S. C. Basaran et al, a unipolar antenna with usage of three-stage microstrip line feeding and CSRR structure was proposed. The resulted antenna was small electrically and the operation bands were 3.5, 2.4 and 5.2 GHz for WiMAX and WLAN applications. The antenna shows that 13, 16 and 17% are the improvement rates of impedance bandwidth [14].
- M. U. Vakani et al. (2012) presented a mini antenna has resonance with more than one band. At first, a square patch antenna with parameters and gain characteristics was analyzed. Then, the SRR structure has employed for the same properties of designed antenna. SRR has the ability to resonate at sub wavelength sizes through effect of LC resonance. It was observed that through scaling the antenna dimensions, the applied SRR structure is small and flexible for designers where antenna can resonate at desired frequency. The results that gave by simple SRR structure compared to conventional square patch antenna showed a reduction rate about 85% of footprint size with gain 1.6dB and bandwidth 5%, structure with strip inside SRR gave a reduction of 94% with gain 1.4dB and bandwidth 6%, while structure with multiple concentric rings has given more bands and 92% size reduction with gain 1.7dB and bandwidth 5.4% and 4.1%. Hence, small sized dual or multi band antenna can be possible with SRR [15].
- In (2012), S. C. Basaran proposed a dual wideband split-ring antenna has a compact size and fed by CPW in order to use it for WLAN applications. The results appear that most or all WLAN operation bandwidths (2.4-2.485 GHz, 5.15-5.35 GHz, and 5.725-5.825 GHz) can be covered by the suggested antenna. Also, the designed antenna can fully meet the demands of interior wireless application through omnidirectional radiation patterns with predicted gains of 5 dBi over the bands [16].
- Y. Dong et al. (2012) designed a compact patch antennas loaded with CSRRs and reactive impedance surface RIS loading. The CSRR structure was integrated on the patch to provide a low resonance frequency where acts as a shunt LC resonator. Employment of diverse configurations of the CSRRs can

produce diversified polarization status with multi-band properties. The components of CSRR and RIS both were able to minimize the antenna size. The CSRR was established on the upper surface as a high-quality factor resonator, excited by effect of the orthogonal electrical field, which can append the field to the patch of antenna for radiating [17].

- W. Cao et al. (2011) displayed a compact low-cost patch antenna with radiation guidance capability. The establishment of CSRR in the ground plane produced a wide-scale orientation domain and also can reduce the cost of a phased array system efficiently in order to achieve the wireless communications requirements. The loading part refractive index impacts the beam direction [18].
- Ó. Quevedo-Teruel et al. (2011) showed a robustly reduction of MPA counted on the SRR structure used. The proposed antenna introduced two simultaneous operating bands by means of its two concentric rings. A parametric study has performed for the operation frequencies to show the rings dimensions effectiveness on them. The results demonstrated that the considerable influence on these resonances has been realized by the dielectric permittivity and total size of the rings. The properties of antenna are highly compact, dual-band and so that can be proper for applications that suffer from size constraints. Substrates with high permittivity have been used for most of the compact antennas. This proposed antenna of this paper presents a compact size with low permittivity substances. New patch antennas that use SSRs have been presented for appointing new bands operate at lower frequencies [19].
- N. Ortiz et al. (2011) showed that a perpendicular polarization can be achieved for double band rectangular MPA through carving a rectangular CSRR on the patch, the CSRR inscription at some patch locations results in reduction of the double band antennas. The chosen design has been come as an alternate resolution for the double-band antenna designs that present these days [20].
- L. Ke et al. (2010) suggested a MPA gives circular polarization by applying single CSRR. The structure of CSRR was formed of mineral slot rings with a merged center and small gap. The radiation patch with engraved CSRR on its

surface was analyzed and fabricated. The prime advantage of this antenna is their little profile and comparatively modest structures, which does not need an exterior polarizer and can be inserted appropriately within the system and equipment that demand compact standard size, such a mobile phone headset [21].

1.2 An important Glimpse of Metamaterial

The focus on the use of metamaterial in recent time has had a clear effect in improving the microstrip antenna function [2-3]. Materials that have negative permittivity and permeability are specified by certain names such as metamaterial, left-handed materials (LHM) and backward wave materials (BWM). The meta-material is of great importance in the conclusion of many theoretical laws even though it does not exist in nature, such as the Doppler Effects, reversal of the Snell's Law, built perfect lenses and Cherenkov radiation [4]. The behavior of slot inside the microstrip patch antenna leads to negative permeability which is collection of shunt inductors with series capacitors [5].

1.2.1 Split Ring Resonator (SRR)

The beginning of interest in various ring and semi-ring structures has been in the early 1950's and for decades with passive permeability were important for synthetic chiral substances as build blocks used in the microwave. SRR is a high-conductivity composition may consist of one or more rings depending on the type of design. Figure 1.1 shows a type of two rings with a required capacitance between them for the induction counter balance [22]. The currents are induced in the rings by applying a vertical and time varying magnetic field on the surface of that rings. These currents produce a magnetic field depending on the resonant characteristics of the structure which may promote or discountenance the accident field leading to negative or positive efficient permeability μ. Employment of SRR also shows the effect of electromagnetic stimulation on materials response [22].

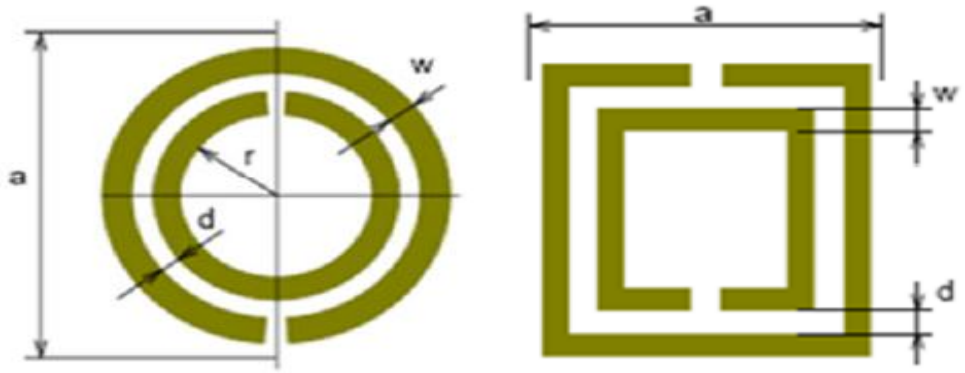

(a) (b)

Figure 1.1 a) circular shape of SRR, b) rectangular shape of SRR [22]

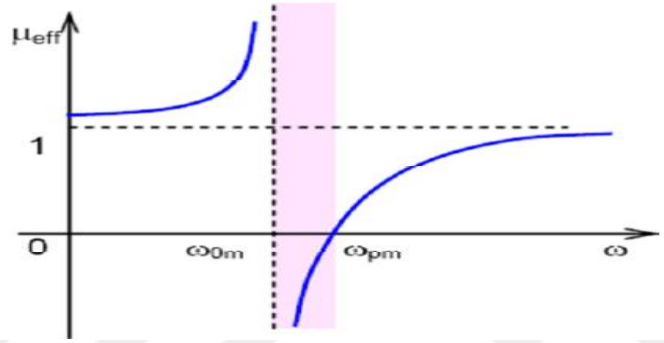

Figure 1.2 Reliance on the frequency of the effective permeability of SRR [22]

Figure 1.2 shows the frequency reliance of μ. The effective permeability is presented to be less than zero with reason of the narrow frequency band and also the expression of $\mu_{eff} \rightarrow \pm\infty$ is particular to the concept of resonant frequencies.

In order to achieve the diversities in the characteristics of the medium there are many adjustments have been proposed for SRR like helical SRR for zero criss-cross polarization [23], for the purpose of increasing the level of non-linear electrostatic effects, the number of azimuth gaps should be increased accordingly, for eliminating the bilateral-anisotropic conduct and to avoid cross-polarization, the non-bilateral differential properties are applied or a wide side conjugate with SRR [24], for the same size there is the possibility to redouble the resonance frequency by doubling the SRR slots, lessening of resonance frequency for the same size by using spiral structures [25], the important resonators for wide bandwidth depend on cross-polarization trends of SRR for frequency selective surfaces [26], reducing the unit

cell size through SRR disfigurement [27], and the filter applications through SRR modification processes [25].

1.2.2 Complementary Split Ring Resonator (CSRR)

Complementary split ring resonators (CSRR) became very diffuse issue in order to realize a multiband microstrip antenna [17]. Depending on the concept of the Babinet's rule that is applied for split rings, the compositions of the complementary dual slit rings are designed and performed [28]. Structures containing slots in the mineral surface, such as the ground plane or the patch and so on are expressed by CSRR as illustrated in Figure 1.3. By the way, CSRRs give negative ε close to the resonance frequency [28].

Figure 1.3 Complementary SRR structures: a) circular, b) rectangular [22]

1.3 Multi-Band Importance for Antenna Applications

Speedy development of the wireless communications has made multiband frequency a necessity for many applications and functions. In addition, the equipment that has this capacity can perform multiple functions at the same time, which may include data transmit, video, audio, radio and so on [5]. In a multi-band antenna, each part operates in a certain range and its gain is below average. It is designed and fabricated to operate from MHz to some GHz.

1.3.1 Global Positioning System (GPS)

GPS is one of the most important applications of the multi-band antennas that fall within the frequency band (1-2 GHz). Compact size of microstrip patch antenna is useful for receiving GPS signals by communication equipment. Since it takes a planar form, and does not expand perpendicularly at the top surface. The radiation

pattern of the microstrip antenna has wide covering with the E-plane at the top of the broadside which permits perfect covering of signals from broadside drop close to the horizon [29].

1.3.2 Worldwide Interoperability for Microwave Access (Wi-MAX) and Wireless Local Area Network (WLAN)

The applications of Wi-MAX and WLAN were assigned for data communication purposes. Wi-MAX has greater coverage distance (around 50 km) comparison with the WLAN (around 30 m). For the purpose of realizing Wi-MAX and WLAN applications there have been a number of designs that suggest the operation of antenna with dual or multi-band characteristics. Operating frequencies of WLAN are (2.4-2.484) GHz, (5.15-5.35) GHz and (5.725-5.825) GHz and Wi-MAX (2.5-2.69) GHz, (3.4-3.69) GHz and (5.25-5.85) GHz [30-31]. There are many proposals, techniques, and structures adopted to obtain a dual-band or multi-band antenna for Wi-MAX and WLAN applications such as the ring patch antenna [32], the monopole antennas and the slot antennas.

1.3.2.1 Double-Broadband G-shaped Slotted Printed Monopole Antenna for Wi-MAX and WLAN Applications

In order to fulfill the worldwide interoperability and the wireless local area network (WLAN) together for microwave access applications of (Wi-MAX), a new double-broadband printed monopole antenna had displayed for this purpose of study. A rectangular monopole antenna was described that has a printed slot like the letter G with defected ground plane for band expansion. FR4-Epoxy as dielectric substrate was used for this antenna. Through describing and illustrating the theoretical and experimental characteristics of the appointed antenna whose selected dimensions are 30 x 48 x 1.6mm3 and the gained impedance bandwidth of 60.26% within the frequency range (2.4-4.47 GHz) and 28.04% within (4.6-6.1GHz), beside a reflection coefficient $\leq$ -10 dBs, It is shown by the characteristics obtained that the operation of the antenna covers a wide range of frequencies including WLAN bands and Wi-MAX bands [33].

1.3.2.2 Multiband Miniaturized Planar Antenna for Wi-MAX, WLAN, UMTS and GSM Bands

In this work, the radiated patch and the ground plane of antenna were exploited by a new technique that used a set of slits and slots to access multiple bands performance. This microstrip compact antenna was designed for contemporary applications of mobile phone and also appropriate for many wireless portable devices. The wireless communication ranges covered by the studied antenna were as follows: PCS (1850–1990 MHz), GSM (824–894 MHz), Wi-MAX [(2.5-2.69), (5.1-5.8) GHz] and WLAN (2.4-2.484 GHz). The empirical results obtained were close to simulated results that showed a good performance of radiant energy in terms of compactness, return loss and gain [34].

1.3.2.3 Broadband and Multiband Monopole Antenna for GSM900 and other Wireless Applications

This study displays the design of a multiband compact antenna with a wide bandwidth. The technique used in this antenna was defected ground structure (DGS) where the broadband and multiband processes were realized through an E-shaped aperture within the ground plane. The current distributions, impedance bandwidth, gain, efficiency and radiation patterns of the antenna were simulated and calculated by measures and computer simulations. Overall size of compact antenna was 30×40×1.57 mm3. There were three distinguished frequency bands for this antenna, centered at 4.75, 2.7 and 0.94 GHz. The bands of frequency can be dominated independently using the parameters of aperture E. [35].

Table 1.1 Wi-MAX and WLAN properties [36]

Specifications	WiMAX	WLAN
IEEE Standard	802.16d,802.16e	802.11
Bandwidth support	3.5MHz,7MHz for 16d(OFDM) 1.75/2.5/3/3.5/5/5.5/7/10MHz for 16e(OFDMA)	20MHz for 11a,20MHz/40MHz for 11n
Frequency bands supported	2.5,3.5 and 5.8GHz supported	2.4 GHz and 5 GHz supported
Data rate	About 70Mbps in OFDM case	maximum supported data rate is 54Mbps in 11a
subcarrier spacing	90KHz for OFDM and 11.16KHz for OFDMA	312.5 kHz
Cyclic Prefix	1/4,1/8,1/16,1/32	same as WiMAX
IFFT point	256 point FFT for OFDM, 128/512/1024/2048 point FFT for OFDMA	64 point FFT including 48 data and 4 pilot carriers,rest guard carriers and 1 DC
MIMO support	Mobile wimax(OFDMA) support MIMO	11n version support MIMO

1.4 Objectives of the Thesis

The aim of survey focuses on three major points:

- The first one is miniaturization the size of the microstrip patch by using Complementary Split Ring Resonator (CSRR), Circular Head Dumbbell Structure (CHDS), Rectangular Ruler Patches (RRPs), Circular Ring Patches (CRPs) and Circular patch (CP).

- The second is design a multi-band rectangular microstrip patch antennas with spacious bandwidth and high return loss, also improvement the performance of Wi-MAX and GPS applications.

- The third is study the behavior of CHDS on three types of conventional antennas, where RIS in this case behaves as main patch of antenna and CHDS as a redirector.

The RISs have used as secondary or additional patches with CSRR and as main patches with CHDS in order to enhance the antenna performance, where CSRR behaves like a metamaterial structure defected from the main patch and CHDS behaves as a redirector.

1.5 Thesis Organization

The research methodology has organized with the following sections:

Chapter 1- Introduction: This chapter presents some techniques, problems, solutions, previous studies and study objectives.

Chapter 2- Antenna Procedures Analysis: This chapter displays some mechanisms, properties and applications of antenna.

Chapter 3- Methodology: In this chapter, the antenna and its associated structures were designed with a discussion and analysis of each case.

Chapter 4- Result and Discussion: In this chapter, all results were presented, discussed and analyzed.

Chapter 5- Conclusion: This chapter contains the conclusions reached through the analytical study of this research.

CHAPTER 2

ANTENNA PROCEDURES ANALYSIS

2.1 General

It is unquestionable that the antenna in term of size has an inverse proportionality with the dependable frequency. For the purpose of radiating high frequency electromagnetic waves efficiently, relatively small sizes of antennas can be designed and used, but with regard to the lower frequencies, it will demand big antennas. The patch is designed in a certain way so that it can radiate. Link the patch to a specific feeder with mutual impedance of 50 ohm. For high polarization with Γ which is generally recognized as the rate of reflected wave to the fallen wave, the transport line is fed at the radiated border provided that the matching between transmitter impedance and antenna impedance is well controlled [37, 38].

2.2 Radiation Mechanization of MPAs

Extension the field between the ground plane and metal of patch can lead to the concept of MPA radiation term. In another way, coupling the MPA to a microwave source leads up to stimulate the patch witch distribute +ve and –ve charges on the superior and minimal surfaces of the patch come along with the ground plane surface. Therefore, the radiation term can be abbreviated as the flowing of the surface current on the mineral patch [32].

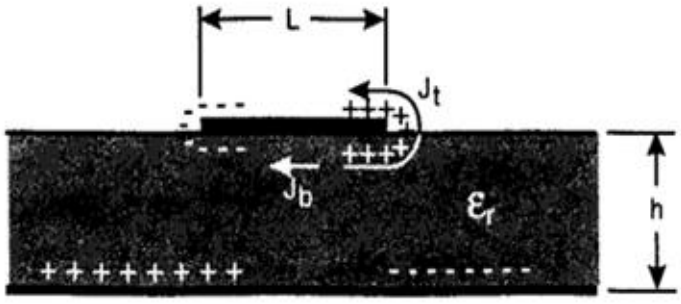

Figure 2.1 The streaming current density with spread of charges on MPA [32]

Phenomenon of charge prevalence implements during the state of domination, where the metal patch is around of half-wavelength. It is known that the identical charges alienate each other and the different charges attract each other. This is exactly what happens to the patch, where each charge on the lower surface of patch begin to repel the adjacent charge, leading to drift of some of the charges that centered on the edge towards the upper surface. Outflow of the charges equalizes the current densities $\overrightarrow{J_t}$ and $\overrightarrow{J_b}$ of the upper and lower patch surface as shown in Figure 2.1. By the way, h/W ratio is very small, where h is substrate thickness and W is the patch width. So, it can be said that the charges will be accumulated beneath the patch, where are accompanied by streaming of current which takes into consideration the importance of attractiveness power between that charges. The weakness of magnetic field that touches the edges of the patch is due to the small amount of current that flows into the top. Therefore, the tangent magnetic field is approximated to zero, while the magnetic effect can be placed over the patch surroundings. Compared to the wavelength, the substrate has very thin thickness ($h \ll \lambda$). Accordingly, the field fluctuations over the height are almost constant and the electric field on the patch surface is fairly normal. As outcome, there is a possibility to design a patch as a cavity with effect of electrical walls and just TM styles are applicable for this case. The electric field distribution of TM_{100} style is shown in Figure 2.2. [32].

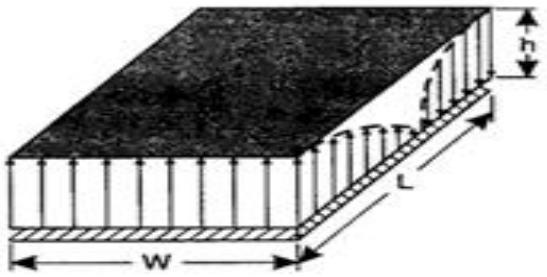

Figure 2.2 Distributed electric field into the microstripe cavity [32]

Radiation is carried out through the four narrow slots of the cavity aspects. Relying on the valence principle of the Huygens field, the microstripe patch can be illustrated through the distribution of current densities on the surfaces. $\overrightarrow{J_t}$ is the current density on the upper face while the four lateral vents are expressed by $\overrightarrow{J_s}$ and $\overrightarrow{M_s}$ densities, conformable to the electric and magnetic fields $\overrightarrow{E_a}$ and $\overrightarrow{H_a}$ respectively [32].

Figure 2.3 (a) clarifies the spread of equivalent currents and is given by:

$$\overrightarrow{J_s} = \hat{n} \times \overrightarrow{H_a} \quad (2.1)$$

$$\overrightarrow{M_s} = -\hat{n} \times \overrightarrow{E_a} \quad (2.2)$$

For fluffy substrate, it turns out that the patch current at the bottom $\overrightarrow{J_b}$ is much higher than the top current $\overrightarrow{J_t}$. It is rounded to zero to denote the lack of radiation and will be neglected from the distributed current. The current density $\overrightarrow{J_s}$ and magnetic tangent field along the edges of patch are also rounded to zero. However, over the patch perimeter, the equivalent magnetic current density $\overrightarrow{M_s}$ is effective and not zero. The illustration is presented in Figure 2.3 (b). Through the image theory, the importance of the ground plane can be observed, which is a significant part in supporting and doubling the magnetic current density. So it can be said that radiation will be confined to the periphery of the patch as radiant strips in free space which is shown in Figure 2.3 (c) [32].

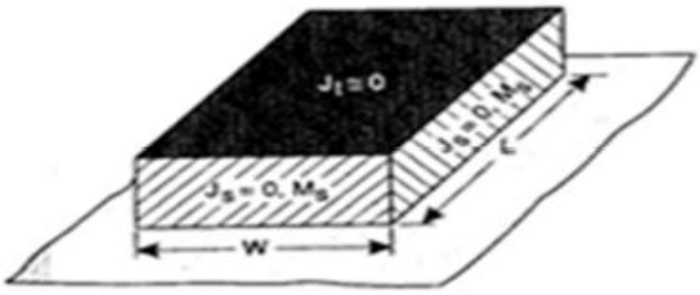

(a)

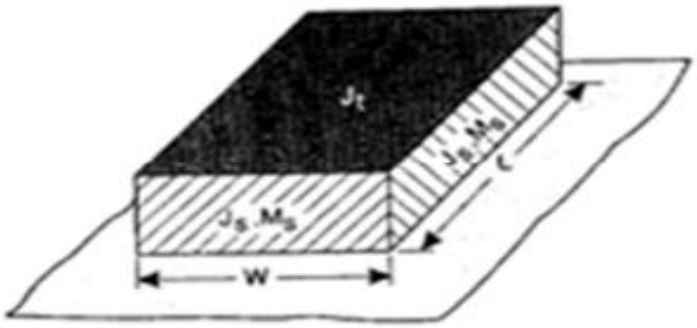

(b)

Figure 2.3 Distribution of equivalent current densities on the surfaces of microstrip rectangular patch: a) M_s, J_s and ground plane, b) ground plane [32]

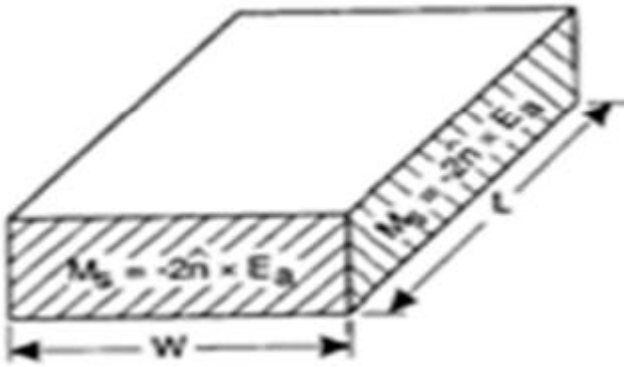

(c)

Figure 2.3 c) Distribution of M_s without ground plane [32]

Current density in magnetic form is given through the new equation:

$$\overrightarrow{M_s} = -2\,\hat{n}\,x\,\overrightarrow{E_a} \tag{2.3}$$

The density of the magnetic current within the apertures will be clarified by Figures 2.4 (a) and 2.4 (b). With looking closely at the principle of equivalence, every one of the vents like a magnetic dipole can radiate the same field beside the current density $\overrightarrow{M_s}$ [32].

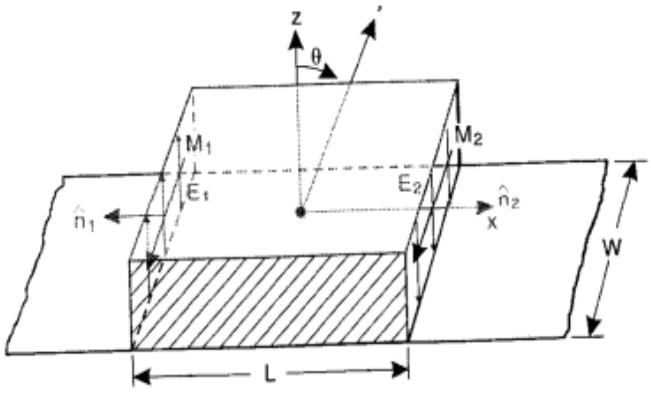

(a)

Figure 2.4 Distribution of magnetic current density on the radiant apertures: a) M_1, M_2, E_1 and E_2 [32]

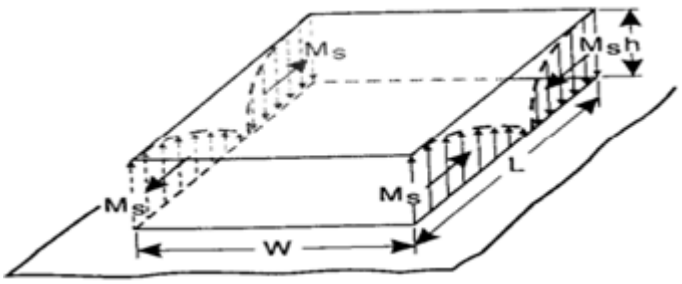

(b)

Figure 2.4 b) Distribution of Current density M_s [32]

The vents that are settled along the x-axis produce a zero-beam due to the distribution of the adverse and equal current on those apertures. On the other hand, two sets of slots are separated through the length of the patch and are located along the y-axis with the flowing current densities that have the same phases and magnitudes. Accordingly, the radiation emitted from the patch can be characterized in expression of two perpendicular apertures [32].

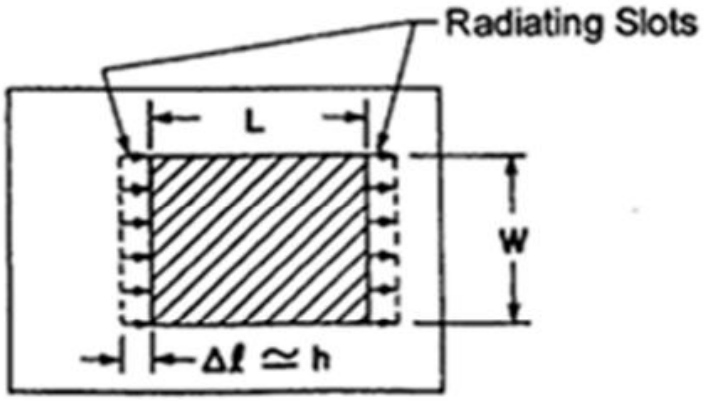

Figure 2.5 Radiant horizontal slots within rectangular MPA [32]

It is very difficult to analyze the vertical apertures in a heterogeneous dielectric of an MPA. So, two planar slots are used instead of vertical as clarified in Figure 2.5.

2.3 Properties of the MPAs

In order to identify the properties of the MPA, several technicalities were suggested and applied, covering the transport line model, multi-port network model and cavity model. One of the most suggested models for MPA is the transmission line. MPA in this model has been presented by two apertures, both have a rise, width and are separated by the length of transport line. The microstrip is simply defined as a heterogeneous line with two insulators that are often substrate and air. Most electric field lines fall within the substrate whereas a few in the air as appeared in Figure 2.6.

Thus, the transmission line is unable to direct a completely pure transversal electromagnetic (TEM) and that because of the diverse phase speeds in the substrate and air. Actually, the quasi-TEM will be the predominant mode of propagation. Accordingly, the wave propagation calculation needs to obtain an effective dielectric constant ε_{reff} [6].

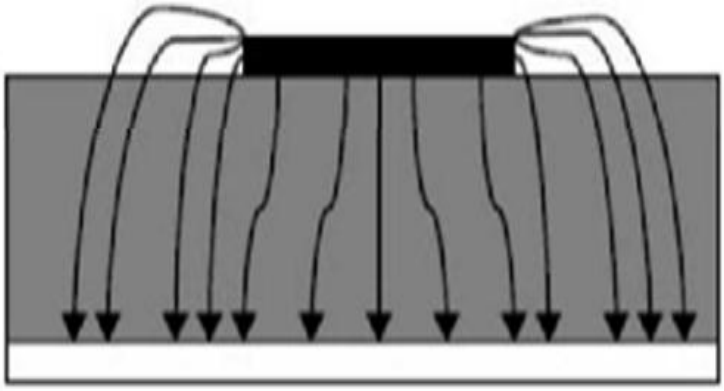

Figure 2.6 Electrical field stripes of MPA [6]

Because the radioactive fields around the patch perimeter are diffuse in the air and are unrestricted by the dielectric, therefore ε_{reff} value slightly lower than ε_r as a comparison between them [2], that as clarified by Figure 2.6.

$$\varepsilon_{reff} = \frac{\varepsilon_r+1}{2} + \frac{\varepsilon_r-1}{2} \left[1 + 12 \frac{h}{W} \right]^{-1/2} \quad (2.4)$$

Where,

ε_{reff} = Effective dielectric constant

ε_r = Dielectric constant of substrate

h = Thickness of dielectric substrate

W = Patch width

Figure 2.7 appears ground plane, substrate with thickness (h) and a MPA with L, W dimensions. The axis of coordination has been chosen in a particular context where the length, width and thickness of the patch are parallel to the directions of x, y and z, respectively [6].

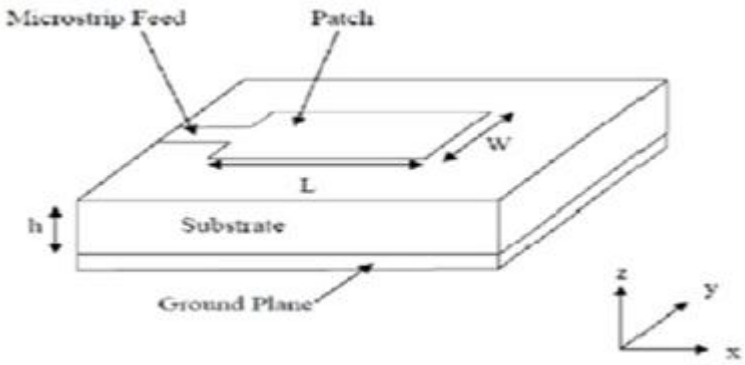

Figure 2.7 Rectangular MPA [6]

The MPA is appeared in Figure 2.8, such as two separated terminal apertures by a length (L) of transmission line. The two terminal ends of patch are open circuits therefore the current along the patch width is very low while the voltage is too high. The edges field effect on ground plane may be set into tangent and ordinary compounds [6].

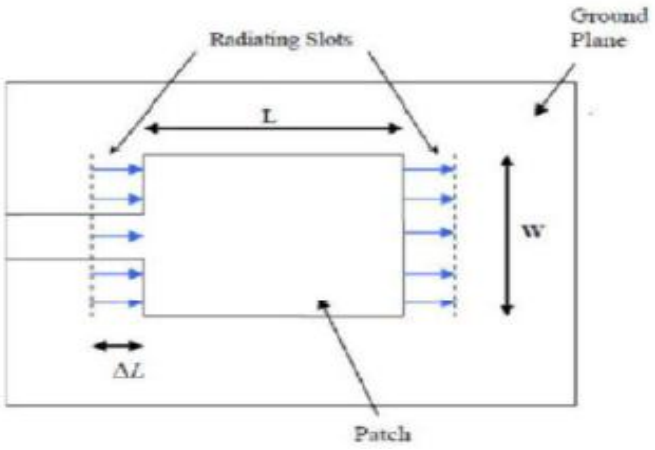

Figure 2.8 Upper face of antenna [6]

The electric field that located at the two edges along the width extension W is divided in a compatible manner into components with adverse directions as appeared in Fig. 2.9. Since λ/2 is the patch length which is accompanied by change of stage therefore that components will abolish each other in the wide side direction. The tangent domains are mutually reinforcing in phase so that the most radiation field is produced toward the composition surface. Through it, the edges that span across the width can act as two radiant apertures that detached by a length of λ / 2 and radiate

over the ground plane in half space with excitation at the phase. The patch electrically looks expanded relative to its real physical dimensions [6]. The patch dimensions have been prolonged now through a distance length ΔL.

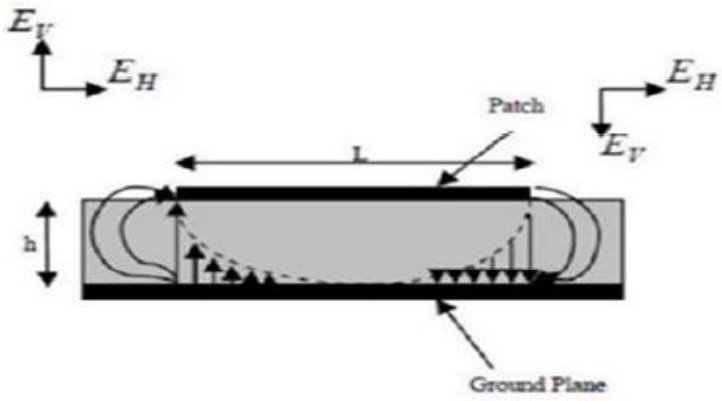

Figure 2.9 Lateral outlook of antenna [6]

$$\frac{\Delta L}{h} = 0.412\ \frac{(\varepsilon_{reff}+0.3)\left(\frac{W}{h}+0.264\right)}{(\varepsilon_{reff}-0.258)\left(\frac{W}{h}+0.8\right)} \tag{2.5}$$

The effective length of the patch L_{eff} now becomes [6]:

$$L_{eff} = L + 2\Delta L \tag{2.6}$$

The frequency at which the MPA resonates is given by

$$f_r = \frac{1}{2L_{eff}\sqrt{\mu_0 \epsilon_0}\sqrt{\varepsilon_{reff}}} \tag{2.7}$$

The width and length of the patch is given by

$$W = \frac{1}{2f_r\sqrt{\mu_0 \epsilon_0}}\sqrt{\frac{2}{\varepsilon_r+1}} = \frac{v_0}{2f_r}\sqrt{\frac{2}{\varepsilon_r+1}} \tag{2.8}$$

$$L = \frac{1}{2f_r\sqrt{\mu_0 \epsilon_0}\sqrt{\varepsilon_{reff}}} - 2\Delta L \tag{2.9}$$

Finally, the length and width of ground is given by [6]:

$$L_g = 6h + L \quad (2.10)$$

$$W_g = 6h + W \quad (2.11)$$

Where,

h = Substrate thickness

L = Length of patch

W = Width of patch

L_{eff} = Effective length

ε_r = Relative permittivity

ε_{reff} = Effective permittivity

2.4 Familiar Techniques for Feeding the MPAs

The salient feeding elements include coaxial feeders, microstrip feeders, aperture-coupled microstrip feeders, proximity-coupled microstrip feeders and coplanar waveguide feeders. Several factors control the choice of feeding technique.

- The effective transmit of power between the radiant structure and feeding element is the most important condition, by meaning, compatibility of impedance matching between the two.
- The reducing of spurious radiance and its influence on the radiation pattern is one of the essential factors for the feeding valuation. The unwanted radiation may raise the side lobe level and the cross-polar amplitude of the radiation pattern [32].

2.4.1 Coaxial Feeding/ Probe Conjugation:

The microwave transmitted power relies on one of the prime technicalities, which is the coupling of power through a probe. The focal coaxial conductor end passes through the substrate then welds with the metallic patch while the second end of the coaxial is linked with the printed circuit board at the back side. The position of the feed point must be specified for the designed work so as to achieve the best impedance matching [32].

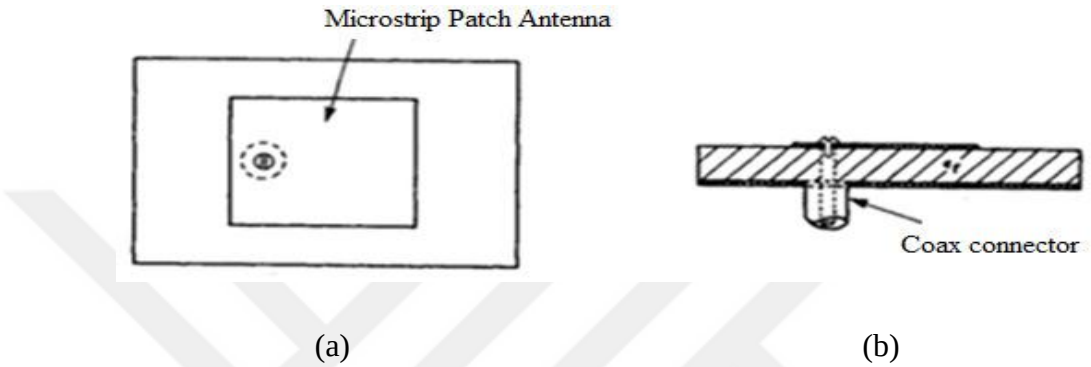

Figure 2.10 A MPA feeding by coaxial probe: a) Upper View, b) Side View [32]

The simple design of coaxial feeding gives an advantage by permitting to select the feed point placement for level amendment of the input impedance. But there are several restrictions. First, makes both industry and the precision of adjustments a difficult issue due to the coaxial feeding requirement for a big number of solder joints. Second, a thicker substrate is used for increased bandwidth of a patch antenna, and that needs longer probe, which causes increase the dispersed radiation from the probe, increase the feed inductance and increase the surface wave power [32].

2.4.2 Microstrip Line Feeder:

This kind of feeding mechanism utilizes a connecting tape that is linked directly to the patch edge as shown in Figure 2.11. The strip conductor in comparison with the patch has small width, and also it can be etched on the substrate as an advantage to provide a planar structure [22].

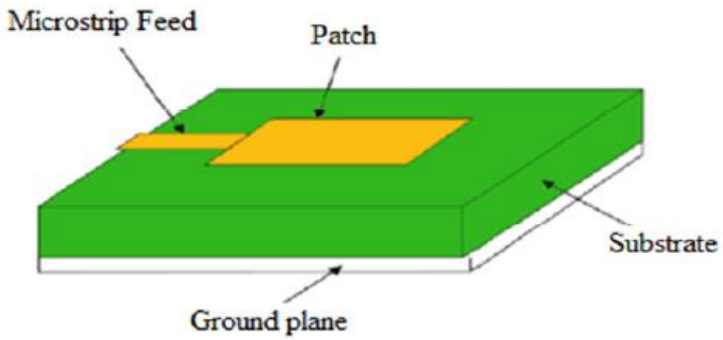

Figure 2.11 Microstrip line feed [22]

The ability of fabrication, forming and simplicity of getting the impedance matching makes this kind of feeding easier to use. Yet, surface waves and radiation dispersed from the feeder will be increased if the thickness of the dielectric was increased, which eventually reduces the bandwidth of antenna. The generating unwanted radiation produces by cross polarized of feed radiation.

2.4.3 Proximity-Coupled Microstrip Feed:

This type is more difficult in fabrication because of its need to provide compatibility between the feeding line and patch. Two layers of dielectric are used to support this type with a patch on the upper layer and a microstrip line on the bottom layer. The end of feeding line is in the open and beneath the patch.

2.4.4 Aperture-Coupled Microstrip Feed:

In this technique a common ground plane is used as a separator between two substrates. The microstrip line of feeding which placed on lower substrate in this case depends on the electromagnetically that can be conjugated to the patch by a slit within the ground plane.

2.4.5 Coplanar Waveguide Feed:

In this method, the feeder radiation will be ignored because of the CPW effectiveness where is excavated inside the ground plane. The microstrip line and coaxial feed have been relied upon. Since, there is a desperate need to get the best impedance matching, coaxial represents the best solution where it is possible to modify the feed point and microstrip feeding line that can be engraved on the substrate with the aim of forming a simple planer antenna [32].

2.5 MPAs Applications

The strong structure and outstanding performance of MPAs make them very important in many applications in various fields such as satellite systems, mobile devices, military systems, medical fields and etc. They are traded commercially and widely due to the low cost of dielectric material of substrate and ease of fabrication. Some of MPA applications are addressed as follows [39]:

2.5.1 Satellites and Mobile Communications:

MPA achieves all the requirements of these applications and are suitable for their design because of its low cost, small structure size and low profile.

2.5.2 Applications of Global Positioning System:

The MPAs provide a very high dielectric permittivity which makes it usable with these applications. These antennas are compressed in size.

2.5.3 Radio Frequency Identification (RFID):

The RFID has been used in several areas such as manufacturing, mobile communications, transportation, health care, logistics and etc. This system ordinarily uses frequency range between (30 Hz and 5.8 GHz) according to the applications [39]. Actually an RFID system can be described as a reader or transceiver and transponder or tag.

2.5.4 Radar Application:

The radars have been employed in order to discover the moveable targets like aircrafts, vehicles, people and etc. The most suitable and optimal choice for radar system demands is MPA, which is easy in fabrication, inexpensive and small in size as mentioned previously.

2.5.5 MPA with Miniature Size for Bluetooth Applications:

In this case, the MPA operates in ISM band from 2400 to 2484 MHz. Though an air substrate is inserted, MPA takes up a tiny volume of 33.3×6.6×0.8 mm3 [39].

CHAPTER 3
METHODOLOGY OF STRUCTURE DESIGN

3.1 Survey of Structure Design

In this chapter, the methodological design of this project will be described which covers metamaterial structures, reactive impedance surfaces (RISs), common conventional and metamaterial antennas emulation. Computer simulation technology microwave studio (CST MWS) has used. In order to reach the desired target, which shows the importance of influential elements or RIS and the significant action of metamaterial in improving the bandwidth and return loss of antenna, there must be an integrated methodology for that, so it will be clarified in Figure 3.1.

3.2 Scheme of Structure Design

The diagram gives a brief overview of the design method, where each influential element is tested with the first and second metamaterials. For metamaterial in this research, the first one is (CSRR) which has good compatibility with MSPA and depends on harmony with the influential element in terms of shape and measurement in order to get good results, the second is (CHDS) which acts as a redirector to exploit the fallen wave in certain applications. This type of metamaterial has the ability to take full control the antenna and handle various types of influential elements used with conventional.

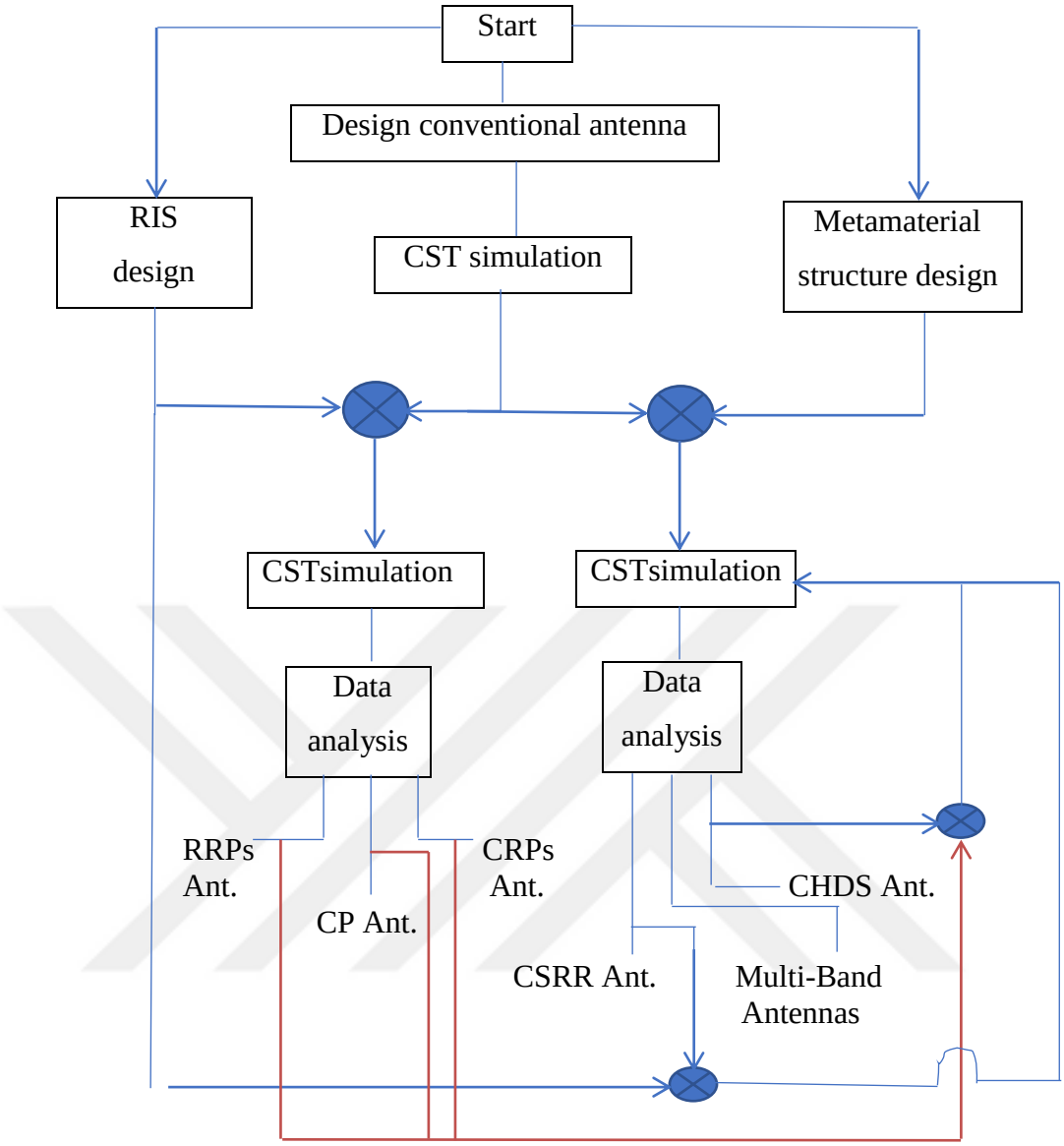

Figure 3.1 Integrated methodology of the study

3.3 Full Antenna Design and Study

The design process in this section will be described in four stages:

- First, conventional antenna or Rectangular Microstrip Patch Antenna design.
- Second, design metamaterial structures and add them to the conventional antenna.
- Third, design influencial elements and add them to the conventional antenna.
- Fourth, collecting the influential elements or RISs with each metamaterial and see the impact on MSPA. As well as the positive effect of the

metamaterials and RISs in optimizing antenna performance and minimizing the size of the patch will be obvious. The difference between CSRR and CHDS in terms of placement that the first one was used as an additional factor to improve the condition of the antenna beside the reactive impedance surfaces (RISs) where the conventional antenna here consists of ground plane, two substrates and patch. The second one was used as redirector for specific applications where the (RIS) here represents the main patch of conventional antenna.

3.3.1 Design Conventional Antenna (MSPA)

The (MSPA) is designed and the simulation is taken at 4.66 GHz and 5.61 GHz in order to be compared with the effect of metamaterials and influential elements. 50 ohm matching impedance also is realized. The example in the figure 3.2 will confirm why impedance matching is essential.

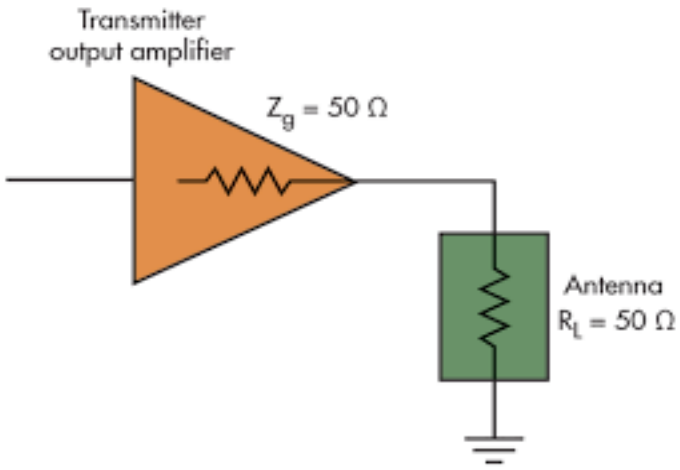

Figure 3.2 Impedance matching [40]

Figure 3.2 shows that antenna impedance must equal the transmitter output impedance and that is considered indispensable to receive maximum power. The transmitter output is usually connected to the antenna via a transmission line, which is typically coax cable. The shape of rectangular microstrip patch antenna will also be shown in Figure 3.3. The characteristics and dimensions of the conventional

antenna will be addressed in the Table 3.1. It is also known that the design of the antenna at operating frequency must have a return loss less than negative 10dB and this condition is achieved in this project in general.

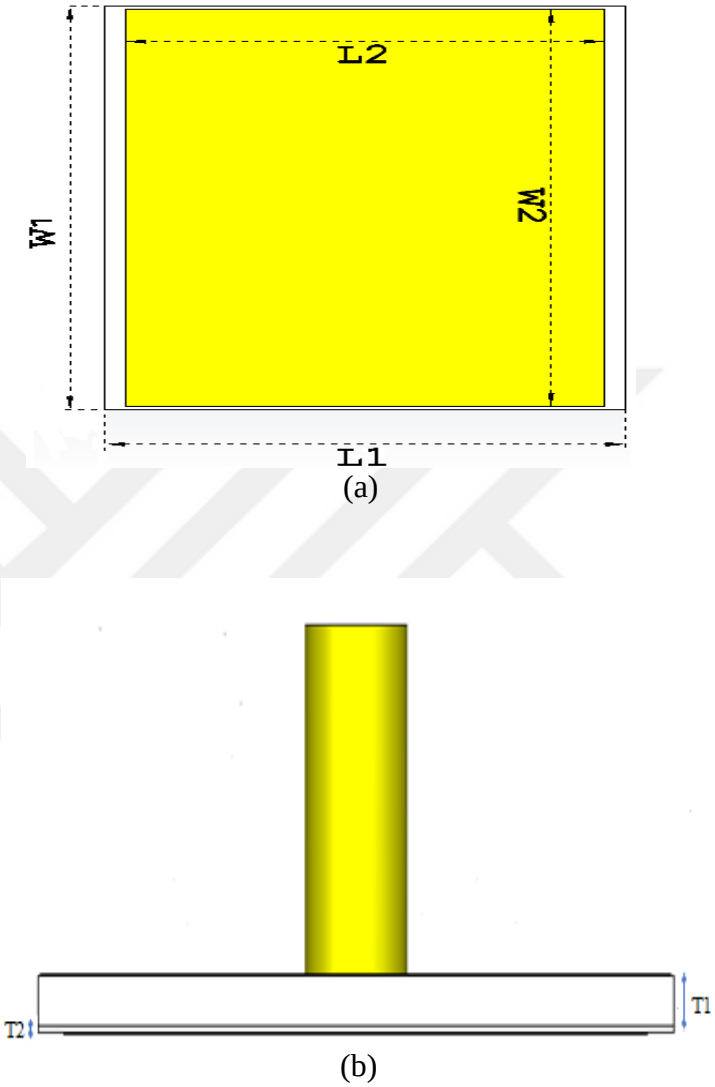

Figure 3.3 Upper and side vision dimensions in (mm) of conventional antenna (MSPA): a) length dimensions, b) thickness dimensions

Table 3.1 Characteristics and parameters of the conventional antenna (MSPA)

operating frequency	4.66 GHz and 5.61 GHz
return loss (dB)	less than -10dB
feeder	coaxial feed
material of patch	Copper (pure)
material of ground	Copper (pure)
material of substrate	FR-4 (Lossy)
effective dielectric constant	4.3
substrate length L1	27 mm
substrate width W1	31.7 mm
patch length L2	24.8 mm
patch width W2	31.2 mm
substrate thickness T1 , T2	1.4 mm and 0.2 mm
patch thickness T3	0.02 mm
ground thickness (t)	0.017 mm

The conventional antenna is simulated to be able to operate at 4.66 and 5.61 GHz as resonant frequencies. Simulation model which used has the following settings as shown in the Table 3.3, mm unit for length and GHz unit for frequency with setting the simulation boundaries of each direction to free space. Antenna perimeter adjusts as open space because these settings are used to calculate the farfield radiation pattern.

Table 3.2 Settings for simulation

length unit measurement	mm
frequency unit measurement	GHz
boundaries	Free space

The feeder used is coaxial feed as mentioned earlier and the simulation frequency was taken from 1 to 10 GHz. Figure 3.4 shows return loss and impedance value of conventional antenna at 4.66 and 5.61 GHz with different probe diameters. Changing the probe diameter of this feeder affects the mutual impedance because the impedance value will change. In the case of the small diameter about 1.2mm, the

return loss is (-13.4dB) at 4.65 GHz and (-13.3dB) at 5.6 GHz with impedance value 53 ohm, but when the diameter is bigger such 1.5mm the return loss is (-11.3dB) at 4.67 GHz and (-10.6dB) at 5.62 GHz with impedance value 44 ohm. The best diameter is 1.3mm which keeps on the impedance value at 50 ohm with return loss (-12.73dB) at 4.66 GHz and (-12.49dB) at 5.61 GHz. So when the diameter decreases, the return loss and impedance value increase and when the diameter increases, the return loss and impedance value decrease. From that can be inferred that the relationship between the diameter on one hand and return loss and impedance value on the other hand is inverse. Also change the diameter of probe less or greater than 1.3mm will make the antenna far from the matching status.

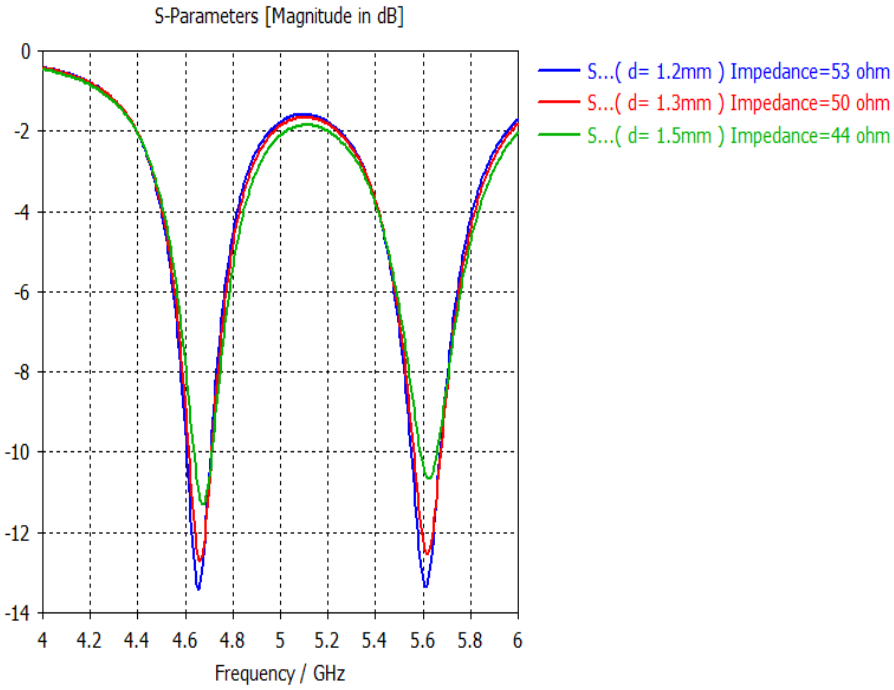

(a)

Figure 3.4 Simulation results of return loss for conventional antenna at 4.66 GHz and 5.61 GHz: a) with impedance value at different probe diameters

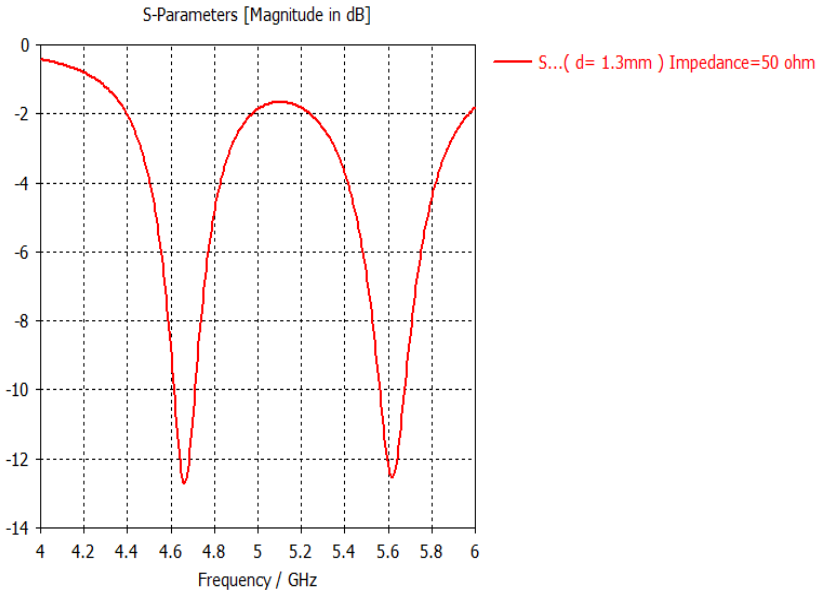

(b)

Figure 3.4 b) Return loss at matching impedance of 50 ohm and 1.3mm diameter

3.3.2 Design (MSPA) with Metamaterial Structures

Two types of metamaterial structures are designed and used with Rectangular Microstrip Patch Antenna. The first one is complementary split ring resonator (CSRR) and the second is circular head dumbbell structure (CHDS). The dimensions of these structures will be clear in table 3.4 and 3.5. Both of (CSRR) and (CHDS) are engraved or defected from the patch.

3.3.2.1 Design Array of 3x3 CSRR

The metamaterial structure CSRR in this study consists of 3x3 single rings as array have the same dimensions and distances between each other. These structures when added to the conventional antenna had a clear effect on improving bandwidth and return loss. The technique of CSRR on the patch performs as a shunt LC resonator for providing a low resonance frequency [17], so it also contributes to minimizing the patch. The compatibility between CSRR and MSPA has occurred. The role of CSRR when locates on the patch surface is like a high-quality resonator excited by the orthogonal electrical field, that can couple the field to the patch for radiance [17]. The shape of the metamaterial structure will display in Figure 3.5.

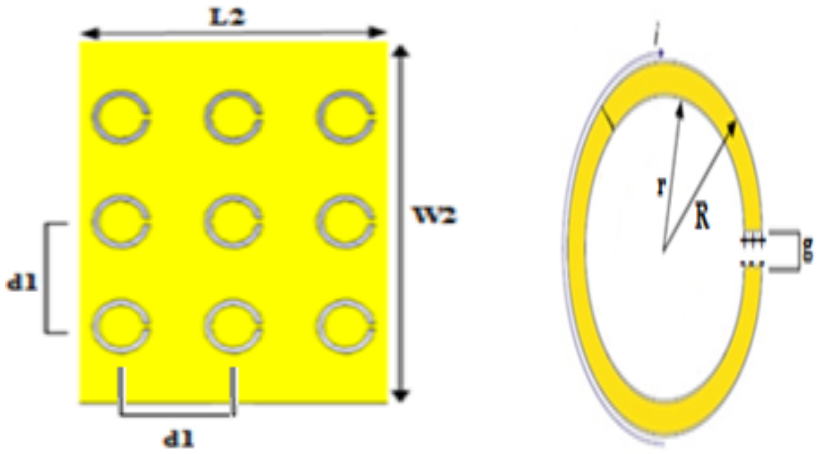

(a) (b)

Figure 3.5 The shape of the metamaterial structure which used with (MSPA) and defected from the patch: a) array of complementary split ring resonators (CSRRs), b) circular split ring

Table 3.3 Dimentions of (CSRR)

distance between rings d1	9mm
g	0.5mm
R	2.3mm
r	1.85mm

3.3.2.2 Design Array of 5x3 CHDS

The metamaterial circular head dumbbell structure consists of 5x3 circles array with slots used for connecting with each other. This structure was used with three types of conventional antennas as redirector, so this structure has the ability to control the properties and applications of the antenna, since it can increase or decrease the bandwidth and return loss as well as minimize the patch size by shift the frequencies and make the antenna operates in certain applications. The effective role of CHDS in collecting and increasing electromagnetic radiation is observed in this study, also its usage in specific functions for WiMAX and GPS applications. The shape of the metamaterial structure will be presented in Figure 3.6.

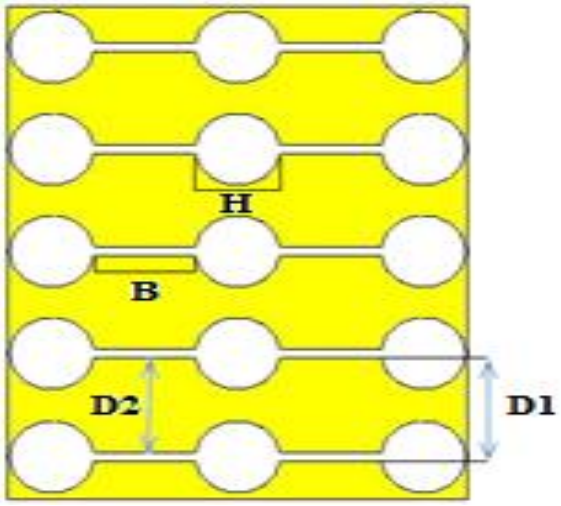

Figure 3.6 Array of CHDS which used with MSPA

Table 3.4 Dimentions of (CHDS)

D1	6.5mm
D2	6.0mm
B	5.43mm
H	4.57mm
radius	2.3mm

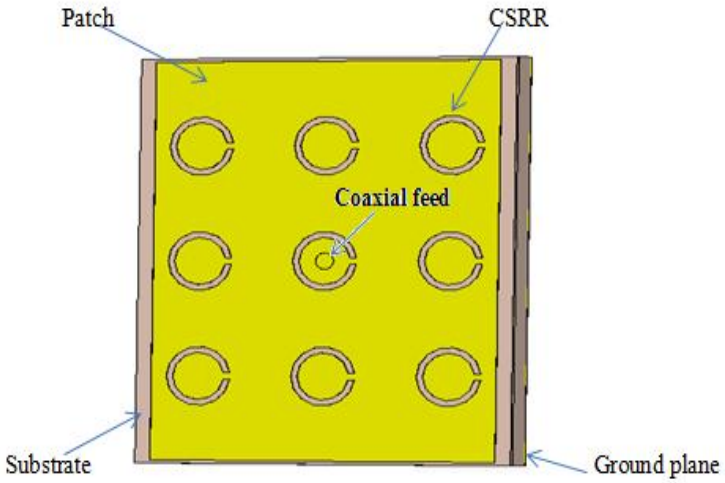

(a)

Figure 3.7 The shapes of the metamaterial antennas: a) CSRR antenna

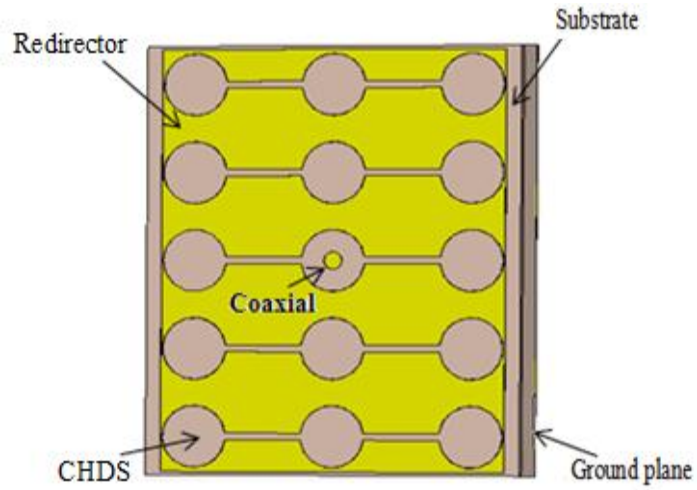

(b)

Figure 3.7 b) CHDS antenna

3.3.3 Design (MSPA) with Influential Elements

Typically, frequency selective surfaces are known as a composite materials designed to be clear in some frequency bands while absorbing, reflective or redirecting to others. They are typically composed of metal and flat shape. In this study, three types of influential elements or RISs were designed and placed between the two substrates of conventional antenna in order to improve antenna performance, which are rectangular ruler patches (RRPs), circular ring patches (CRPs) and circular patch (CP).

3.3.3.1 RRPs and CP Elements

RRPs consist of 15 rectangular patches located like horizontal rows between the two substrates. CP is a single circle located between the two substrates. The effect of rectangular ruler patches and circular patch was positive in improving bandwidth and return loss. The return loss is represented by the ratio of reflected power to input power (Pr/Pi), so the output or reflected power of antenna will increase by using RRPs or CP. In general, a small or large shift of frequencies may occur when using additional structures with the antenna. However, it will be noticed in the results chapter that these structures have not caused significant shift for frequencies with the creation of an extra band by CP and that relates to the concept of selectivity, where the energy must be absorbed and/or redirected for frequency selectivity or filtering [41]. The extra frequency band of CP gave a good reduction to the size of the patch,

which will be observed in Chapter 4. The sections (c) and (d) of figure 3.8 show that field lines are perpendicular to the surfaces of the circle and straight rod at every point [42]. The created magnetic field lines become closer together and result in an intensity of the magnetic field at the middle section [42]. According to Faraday's law, the changing in magnetic field at the end will induce an electromagnetic field that leads to create a new magnetic field which is opposed to the change in that field. This will cause interference between the two magnetic fields, leading to the new form of reflected power and frequency selectivity [41]. Also with high matching impedance between the transmitting and feeding, the return loss and bandwidth of antenna will be increased.

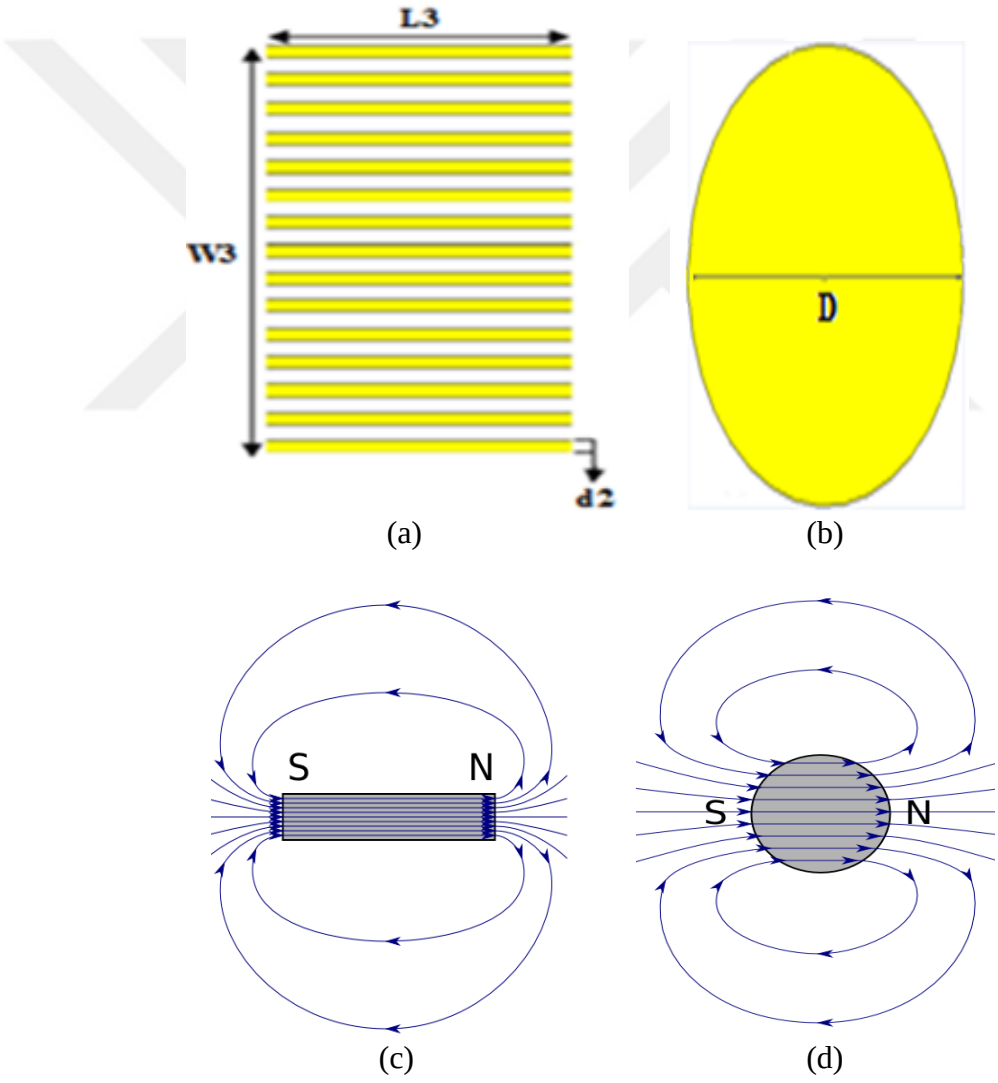

Figure 3.8 The shapes of the RISs with distribution of magnetic flux:
a) RRPs, b) CP, c) magnetic field lines of straight rod [42],
d) magnetic field lines of circle [42]

Table 3.5 Dimentions of RRPS and CP

material of RRPs and CP	copper pure
d2	1mm
L3	25mm
W3	29mm
diameter of CP (D)	18mm
RRPs and CP thickness	0.017mm

3.3.3.2 CRPs Elements

CRPs consist of 9 rings as array 3x3 located between the two substrates. This rings had a slightly negative effect by reducing bandwidth and return loss of MSPA. The main reason is that the applied rings cause absorption and dissipation of some input power to reflect less power. The dielectric permittivity, elements spacing, angle of wave incidence and the overall rings size have a considerable effect on the resonances [19]. Energy absorption is not always a negative matter for antennas, sometimes it is invested for specific applications in aircraft, ships and so on [41]. It will be observed later on how this effect is exploited by CHDS redirector in WiMAX and GPS applications. Figure 3.9 illustrated the shape of these influential elements with their dimensions and distribution of magnetic field lines.

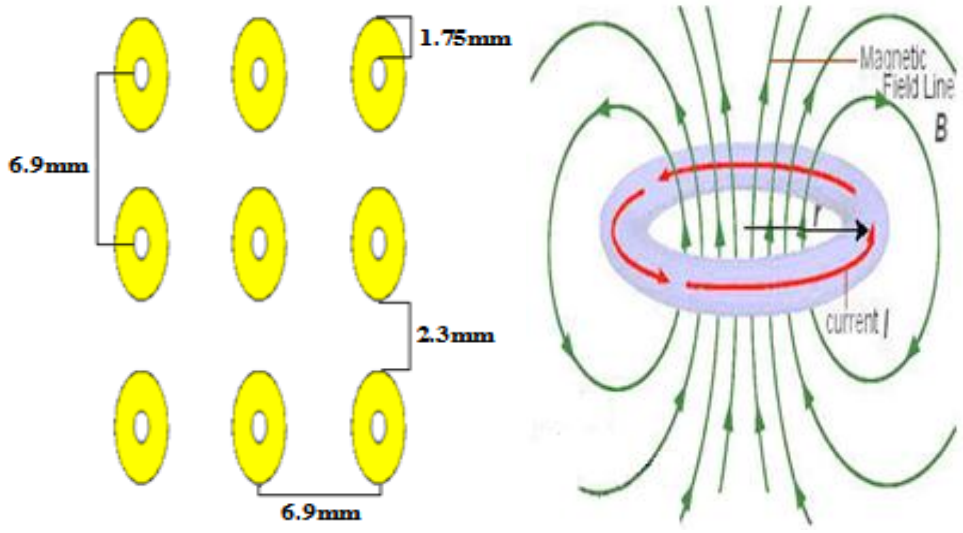

(a) (b)

Figure 3.9 The shape of the RIS with distribution of magnetic flux:
a) CRPs, b) magnetic field lines of circular ring [43]

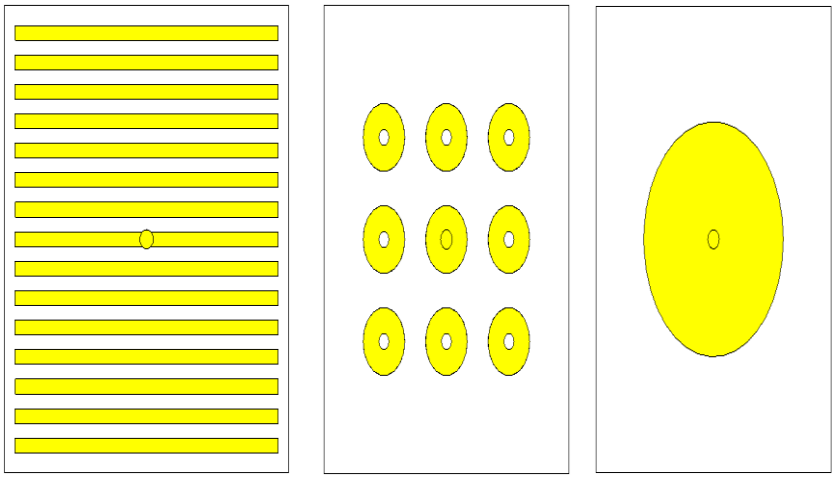

Figure 3.10 The inside view of RISs shapes incorporated with conventional antenna: a) RRPs antenna, b) CRPs antenna c) CP antenna

It is important to mention that these RISs act as additional influencing elements for the traditional antenna when employing the structure CSRR, but behave as part from traditional antenna or the main patches when CHDS is used.

3.3.4 Full Antenna Design with Metamaterial and Influential Elements

In this part, metamaterials and influential elements will be incorporated with the conventional antenna to build an integrated antenna which represents the last model of antenna design. Several objects will be discussed in this section of the chapter that include the results of combining these RISs with the metamaterials in order to show the reaction on the antenna. Six cases of an integrated antenna are presented and each case will be discussed separately:

- The first case involves the insertion of RRPs with CSRR.
- The second case involves the insertion of RRPs with CHDS.
- The third case involves the insertion of CRPs with CSRR.
- The fourth case involves the insertion of CRPs with CHDS.
- The fifth case involves the insertion of CP with CSRR.
- The sixth case involves the insertion of CP with CHDS.

3.3.4.1 First Case (RRPs with CSRR)

As aforementioned, the effect of (RRPs) element and (CSRR) metamaterial was positive in expanding the bandwidth and improving return loss of conventional antenna. Inserting them together with the conventional antenna has generated four bands instead of two to make the antenna operate at 4.36 GHz, 4.7 GHz, 5.6 GHz and 5.99 GHz with high return loss, so that represents an advantage for this antenna. The CSRR metamaterial absorbed the power produced by the RRPs effect to redirect it with two extra bands and with higher reflection for radiation power. The created frequency band 4.36 GHz gives a minimization in the size of the patch. The frequency resonators depend on the angle of energy wave incidence and the spacing between metamaterial rings, according to [41]. The length, width, number of rulers and distance between them for (RRPs) represent the best measurements according to the results. The changing in some of that dimensions reduced the return loss of all bands with the emergence of a new band at GPS frequency range. The new band in this case caused a high miniaturization for the patch and that from the desired goals. Figure 3.11 will display steps of access to the integrated antenna.

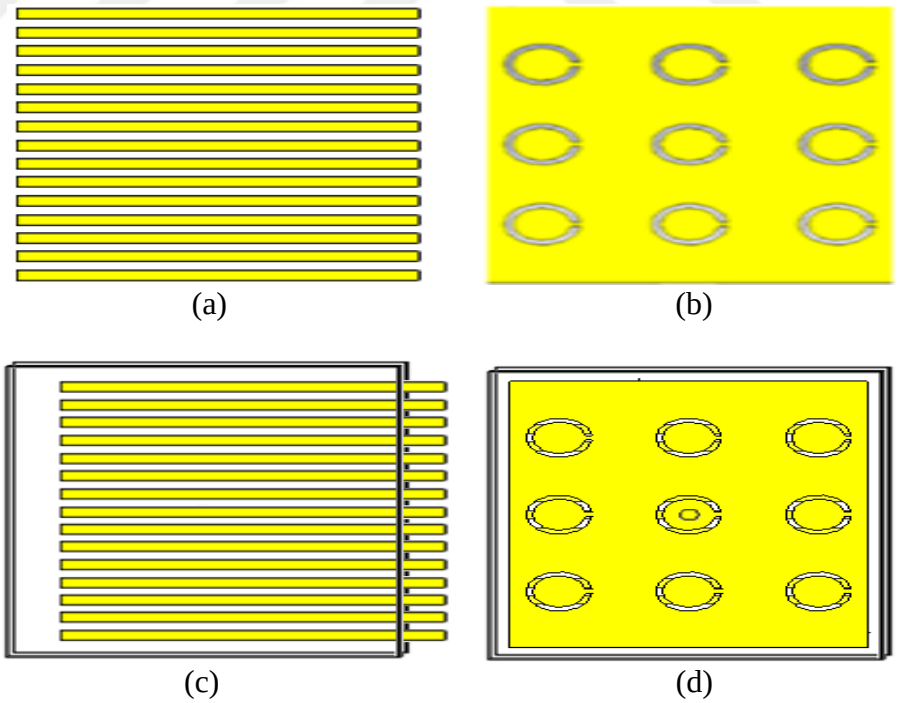

Figure 3.11 The stages of integrated antenna construction: a) RRPs, b) defected patch for CSRR, c) insert RRPs between the two substrates, d) integrated antenna

3.3.4.2 Second Case (RRPs with CHDS)

Despite the positive effect of the (RRPs) on conventional antenna at 4.6 GHz and 5.58 GHz, the incorporation of RRPs and CHDS in the same antenna led to removal of one of the bands as well as reduce the second bandwidth and return loss in comparison with effect of RRPs only. The behavior of CHDS redirector in this case showed a high dispersion of energy with a sharp drop in reflection. Anyway, that behavior will be studied in chapter 4. Figure 3.12 shows stages of access to the integrated antenna.

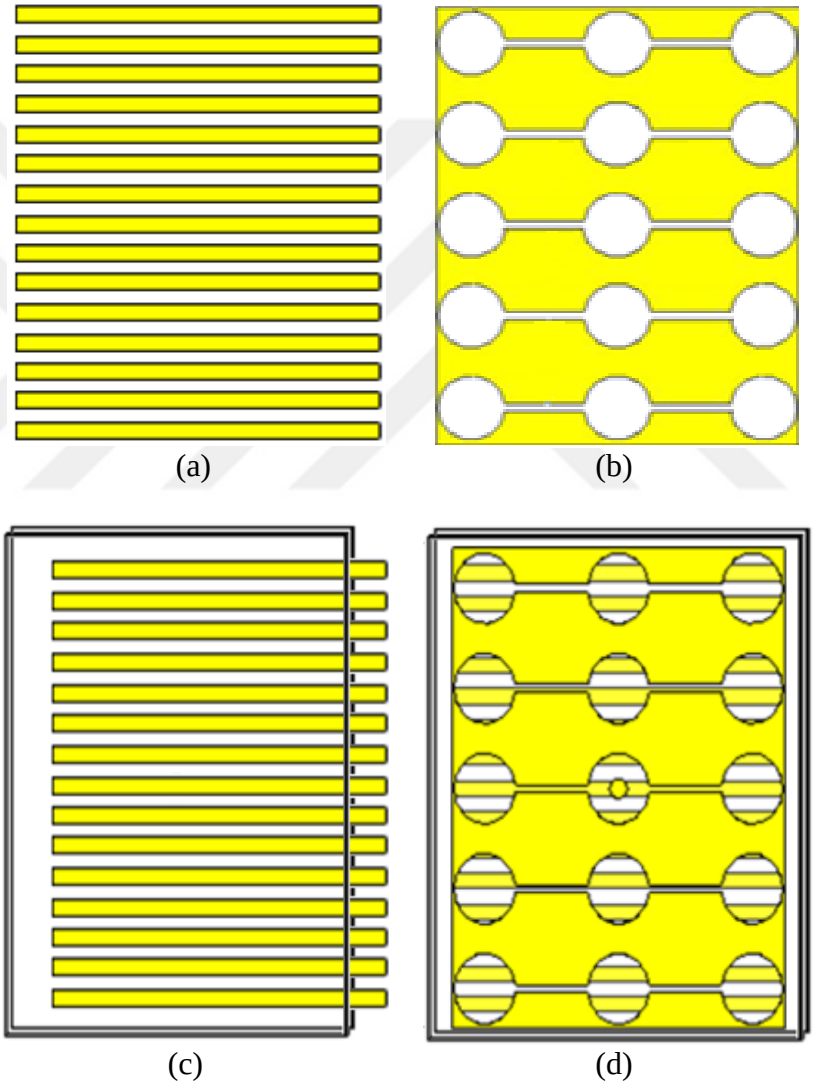

Figure 3.12 The stages of integrated antenna construction: a) RRPs, b) CHDS redirector, c) insert RRPs between the two substrates, d) integrated antenna

3.3.4.3 Third Case (CRPs with CSRR)

Conventional antenna plus (CSRR) metamaterial operates at 4.4 GHz and 5.24 GHz with good improvement. In this case the influence was reducing the number of bands to make the antenna work at 4.52 GHz only. This type of metamaterial depends on the amount of energy that falls on it, the incidence angle and the dimensions of rings. Therefore, CSRR behavior was due to the low energy of CRPs, also after changing the radius of (CRPs), radius of (CSRR) and the distance between rings of (CRPs), the second band returned and the antenna operated at 4.51 GHz and 5.46 GHz with reduction in bandwidth and return loss compared with effect of CSRR only. Figure 3.13 will show steps of access to the integrated antenna.

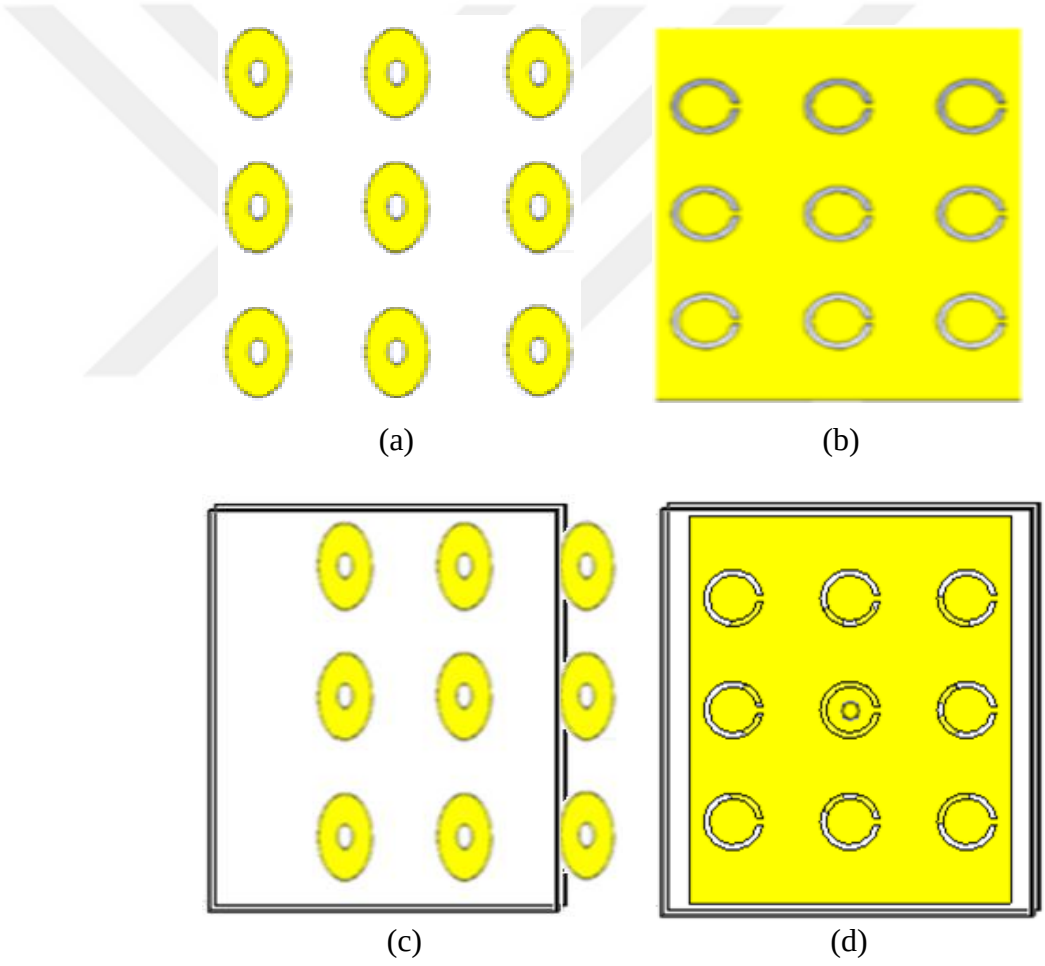

Figure 3.13 The stages of integrated antenna construction: a) CRPs, b) defected patch for CSRR, c) insert CRPs between the two substrates, d) integrated antenna

3.3.4.4 Fourth case (CRPs with CHDS)

This case shows the positive effect of redirector (CHDS) on CRPs antenna. In spite of the negative effect of CRPs on MSPA, its merging with CHDS into the same antenna gave good results. The integrated antenna operates at 5.68 GHz and 1.55 GHz with high return loss and enhanced bandwidth with a significant miniaturization for the patch. Sometimes, the negative reaction of these structures may be a reason for achieving good results. The good results obtained are not only due to the harmonic factor but because of the dominant behavior of this redirector which will be studied with simulation results in Chapter 4. Figure 3.14 appears the steps of access to the integrated antenna.

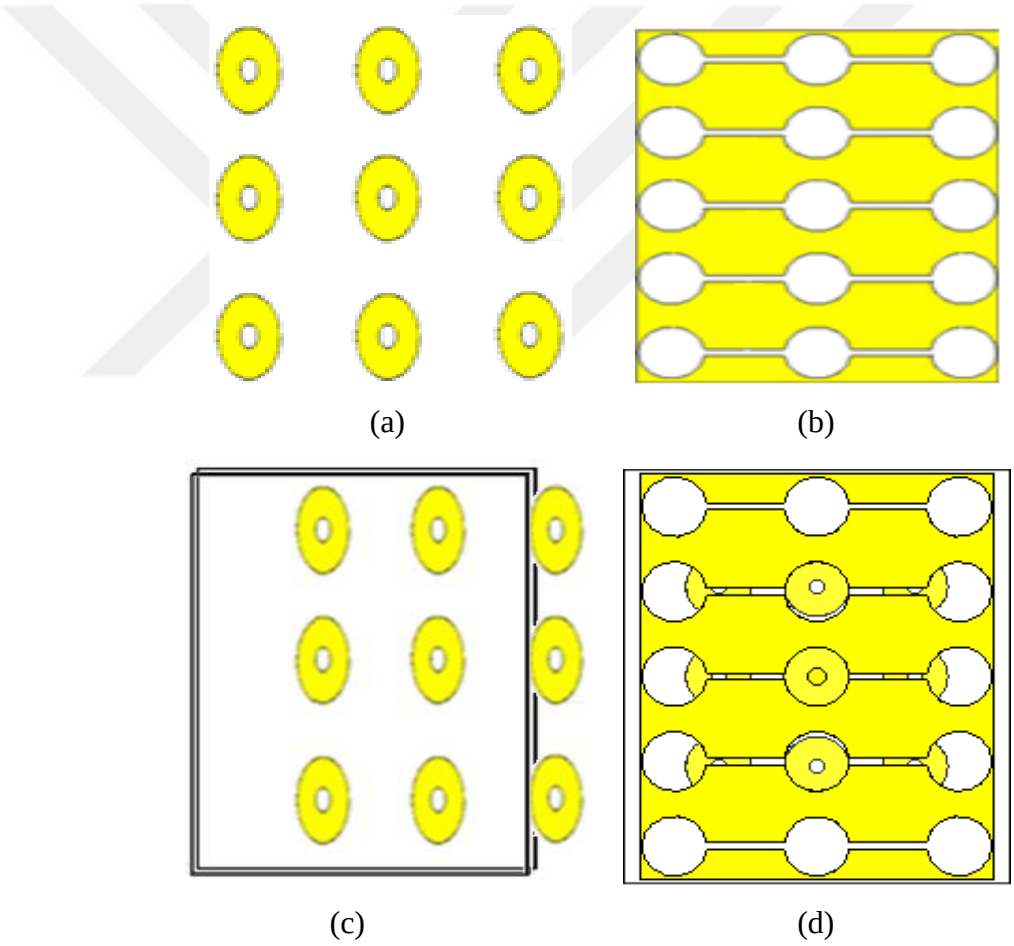

Figure 3.14 The stages of integrated antenna construction: a) CRPs, b) CHDS redirector, c) insert CRPs between the two substrates, d) integrated antenna

3.3.4.5. Fifth Case (CP with CSRR)

Adding CP with the conventional antenna showed a clear effect in improving the bandwidth and return loss. In particular increase the number of bands to make the antenna operate at 5.65 GHz, 4.69 GHz and 2.66 GHz with high return loss. The frequency band 2.66 GHz gives high reduction in patch size. The good results depend on the diameter of the CP, less or more than 16mm make the return losses start to fall. The effect of CSRR also depends on diameter of CP, as example at D=16mm the return losses reduced but at D=26mm the return loss and bandwidth were improved although 26mm had a much lower impact than 16mm on the conventional antenna. So the behavior of this type of metamaterial varies according to the change in dimensions of RISs and requires compatibility with influential element to obtain good results. It can be noted that CSRR metamaterial has an opposite behavior in comparison with the CHDS which is not affected by the change in dimensions but instead of that imposes its influence on antenna in general. Figure 3.15 appears the steps of access to the integrated antenna.

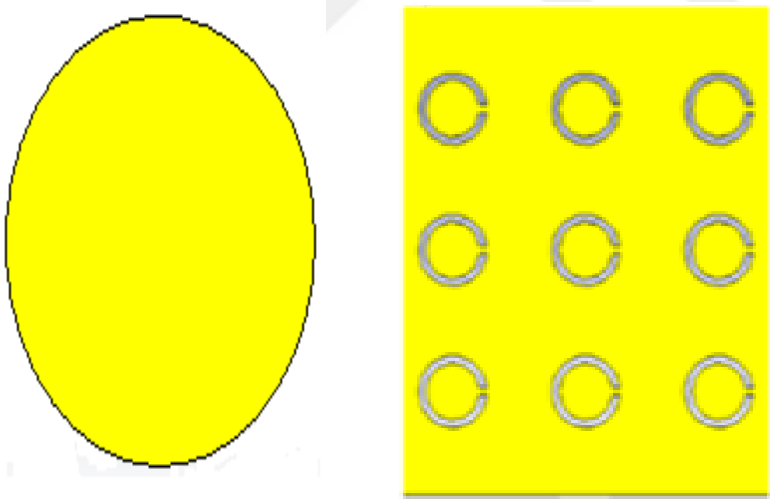

(a) (b)

Figure 3.15 The stages of integrated antenna construction: a) CP, b) defected patch for CSRR

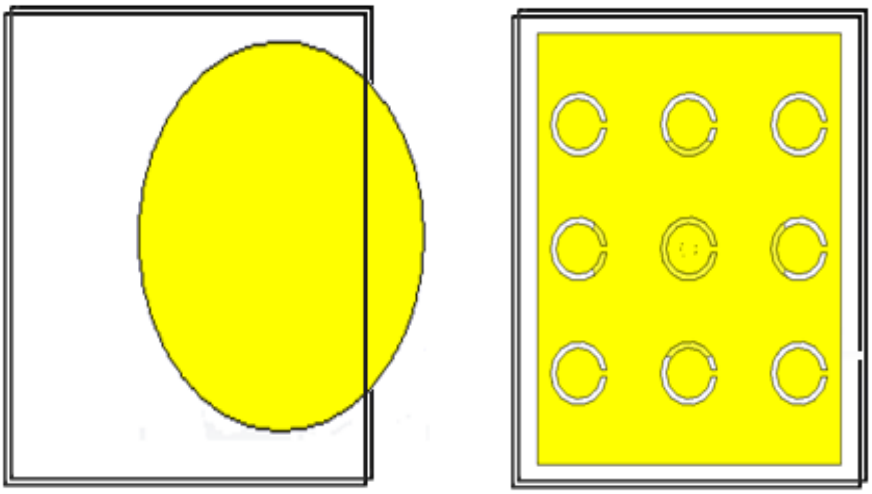

(c) (d)

Figure 3.15 c) insert CP between the two substrates, d) integrated antenna

3.3.4.6 Sixth case (CP with CHDS)

Merging CP and CHDS into the same antenna clarified much of the CHDS strategy where its behavior does not change even with change of CP diameter. The behavior of this structure is positive for some frequencies, which significantly increases return losses and bandwidth and negative for other frequencies where it removes a full band of those frequencies. Through the results obtained, the fixed behavior of the CHDS strengthens the WiMAX and GPS frequencies, but not in all cases there are certain conditions for its behavior will be explained in detail in the results chapter. Figure 3.16 appears the steps of access to the integrated antenna.

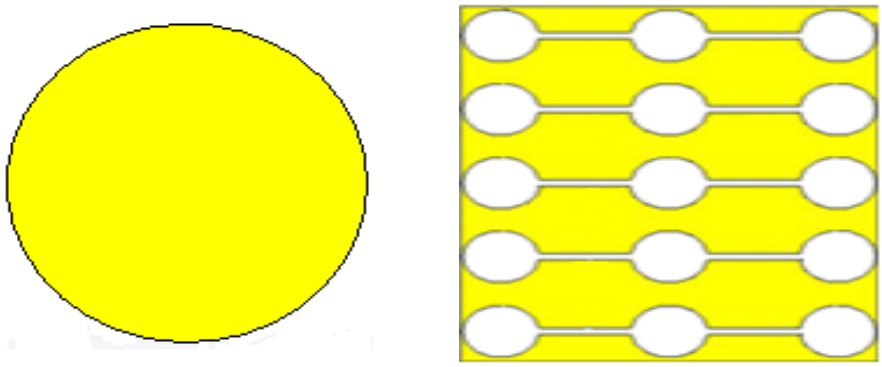

(a) (b)

Figure 3.16 The stages of integrated antenna construction: a) CP, b) defected patch for CHDS

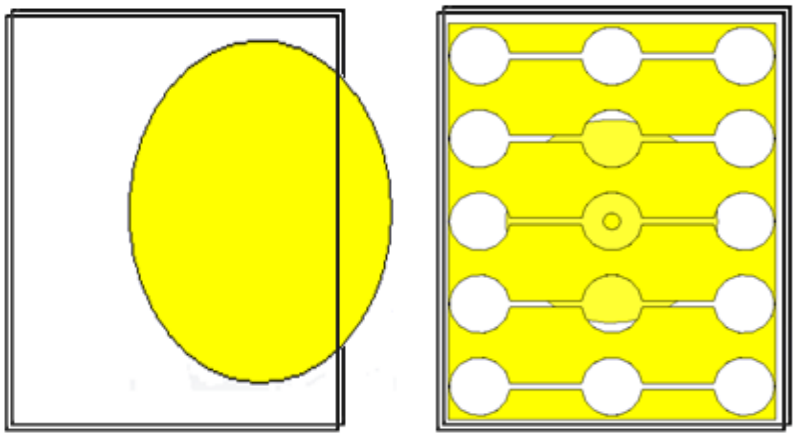

(c) (d)

Figure 3.16 c) insert CP between the two substrates, d) integrated antenna

CHAPTER 4
RESULTS AND DISCUSSION

4.1 Introduction

The microstrip rectangular patch antenna with two types of metamaterials and three types of influential elements were designed in Chapter 3. The method of design and synthesis has been clearly explained with figures and tables. In this chapter the results and comparisons between (MSPA) and effect of other structures will be presented.

4.2 Comparison between the Previous Work and the Current Work by CST Program

In this section, there will be a comparison between my work and previous work, which is (Design and Characterization of Miniaturized Patch Antennas Loaded with Complementary Split-Ring Resonators) [17].

4.2.1 Configuration

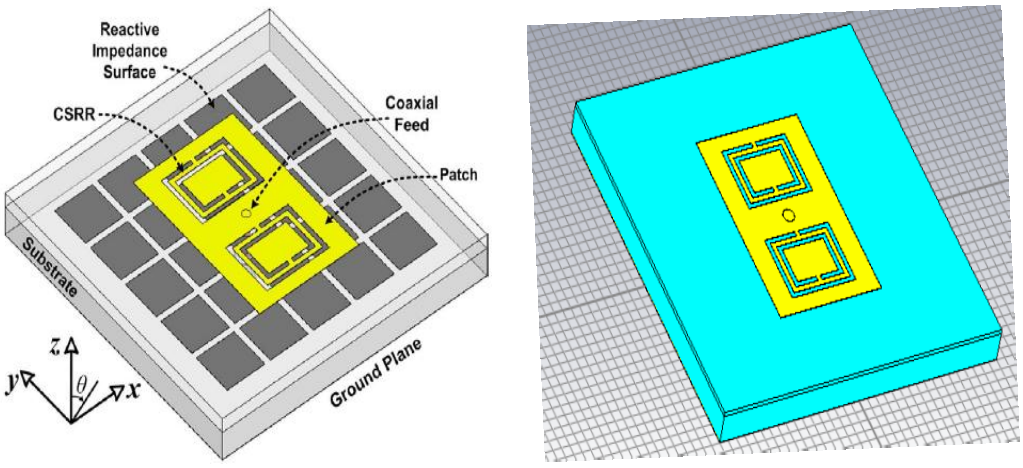

(a) (b)

Figure 4.1 Configurations of the proposed CSRR-loaded patch antenna over an RIS: a) Perspective view of [17], b) current work

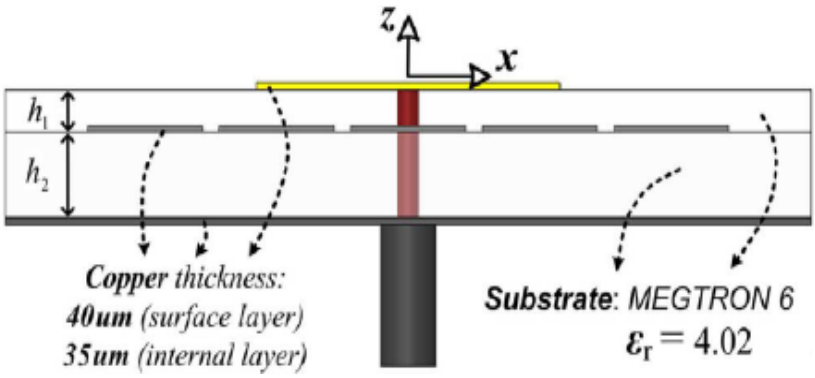

(c)

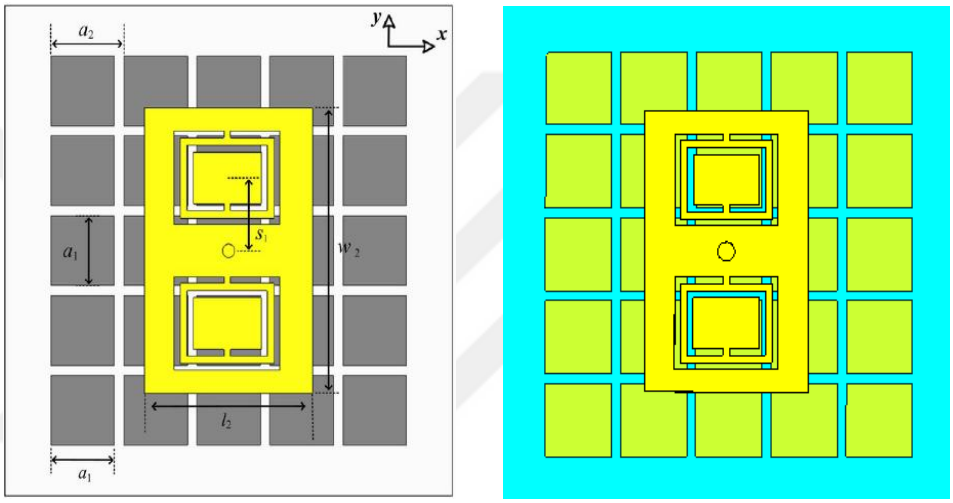

(d) (e)

Figure 4.1 c) side view of [17], d) top view of [17], e) top view of current work

4.2.2 Simulation Results

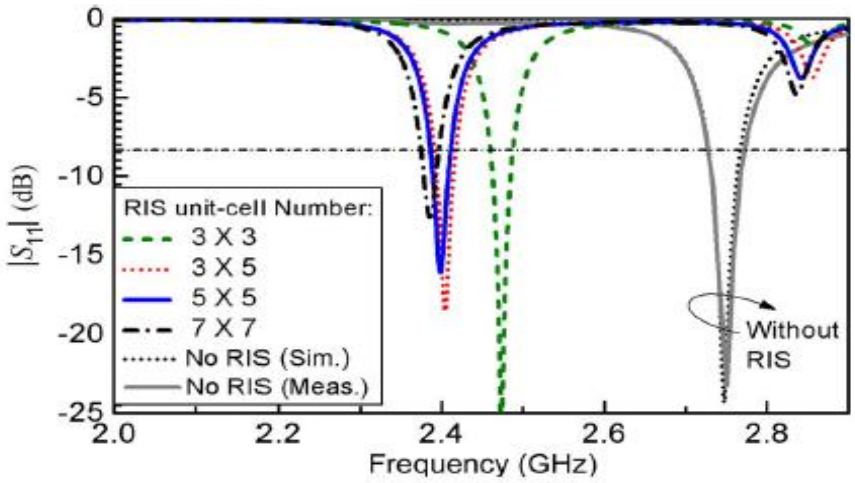

(a)

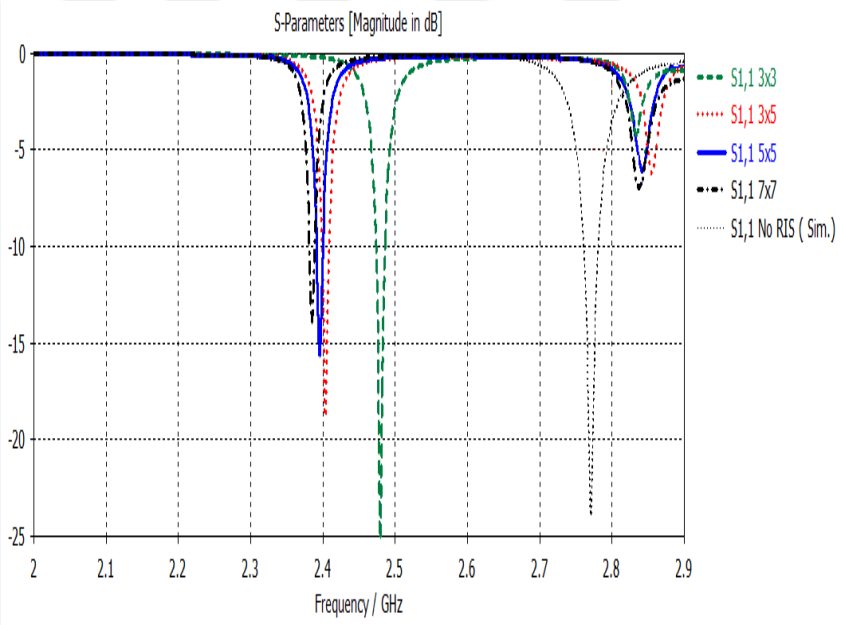

(b)

Figure 4.2 Comparison of simulation results at various numbers of RIS: a) [17], b) current work

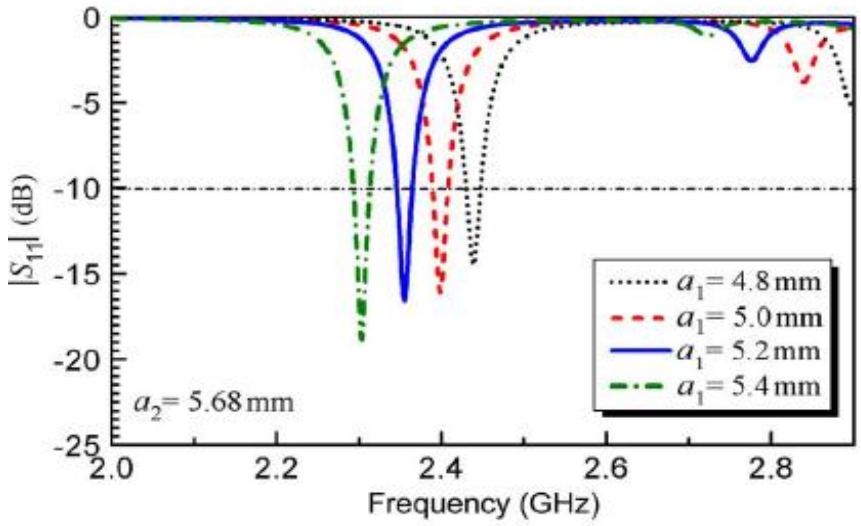

(a)

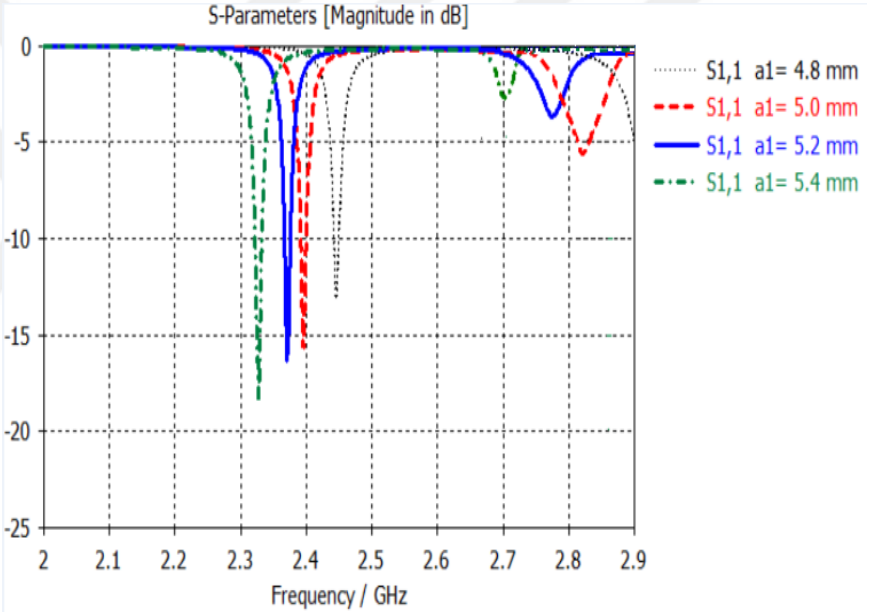

(b)

Figure 4.3 Comparison of simulation results at various dimensions of RIS: a) [17], b) current work

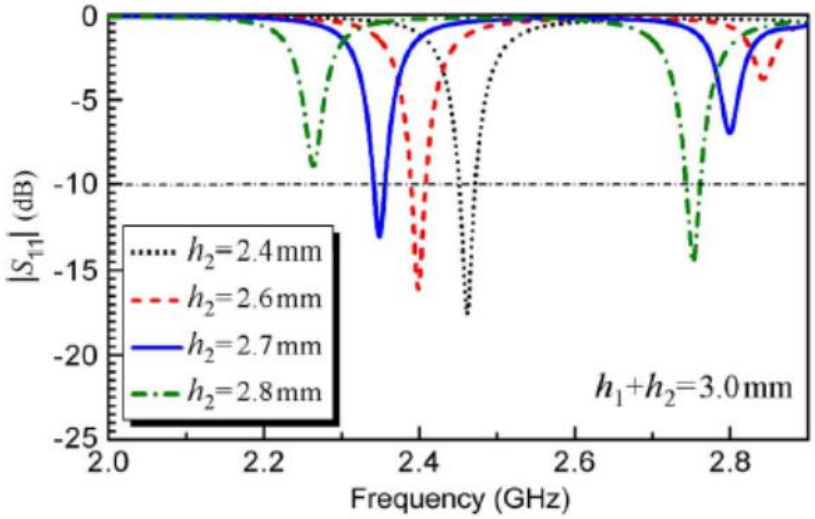

(a)

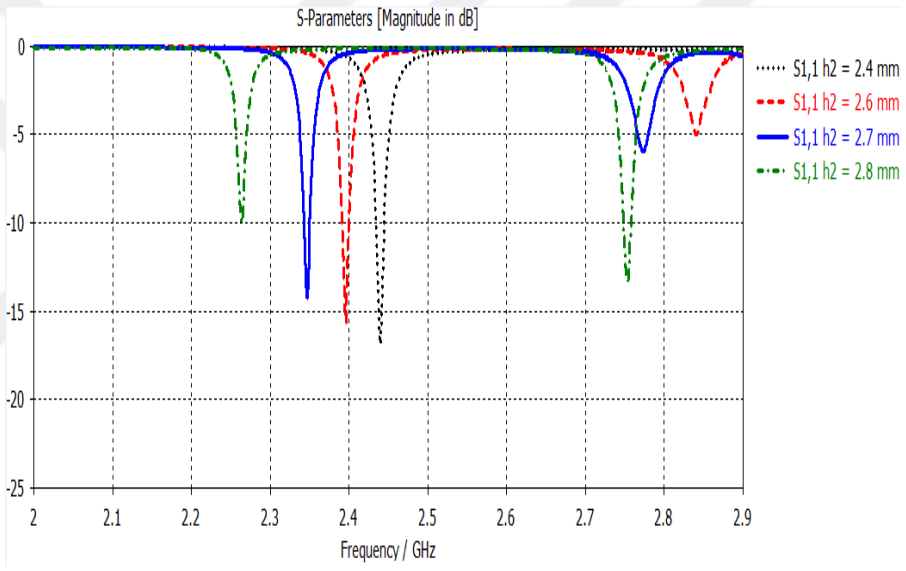

(b)

Figure 4.4 Comparison of simulation results at various thicknesses of substrate: a) [17], b) current work

Through the comparison, it was noted that the results were very close and thus will be as backing for the new work.

4.3 MSPA with RISs at 4.66 GHz and 5.61 GHz

This section includes a comparison between the conventional antenna and the influence of elements at 4.66 GHz and 5.61 GHz. The simulation of all were taken to display the difference in terms of bandwidth, return loss and radiation pattern.

4.3.1 MSPA with RRPs Effect

Through simulation results the impact of RRPs in increasing the return losses and bandwidth was obvious.

4.3.1.1 Return Loss Simulation

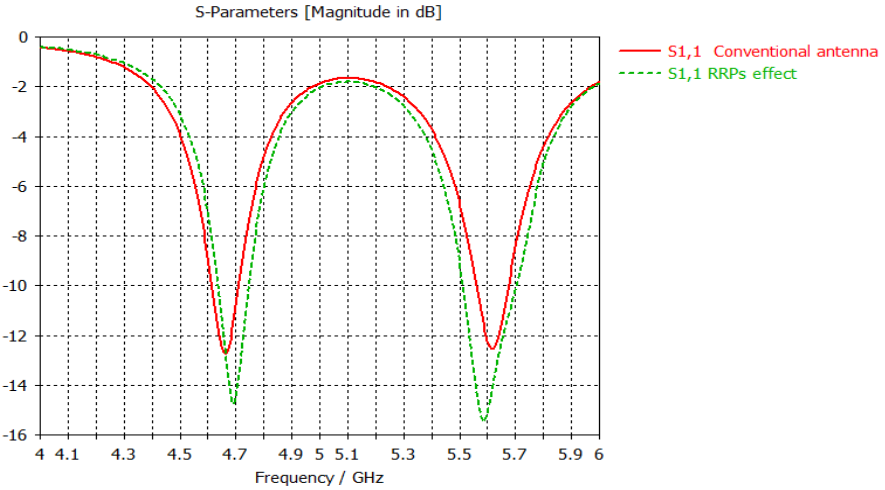

Figure 4.5 Comparison of return losses between MSPA and RRPs antenna

Figure 4.5 appears the return loss curve S1,1 of the conventional antenna compared to the return loss curve S1,1 of RRPs. It is clear now that inserting RRPs with conventional antenna gives better results by raising the return losses to -14.7dB and -15.4dB at 4.68 GHz and 5.58 GHz respectively compared with results of conventional without RRPs which are -12.7dB and -12.5dB at 4.66 GHz and 5.61 GHz respectively. Note that RRPs causes slightly shifting in frequencies of MSPA about 20 to 30 MHz. The operating bands of antenna with RRPs are between 4.636 GHz to 4.745 GHz and 5.512 GHz to 5.704 GHz, so bandwidths of RRPs-effect antenna are 109 MHz at 4.68 GHz and 192 MHz at 5.58 GHz compared with conventional antenna which has lower bandwidth about 95 MHz at 4.66 GHz and 114 MHz at 5.61 GHz. So with RRPs, the bandwidth increases by 14% and 68% respectively.

4.3.1.2 Radiation Pattern Simulation

3D radiation pattern and polar plot for both conventional antenna and RRPs-effect antenna were simulated. The simulating results appear in Figure 4.6, where (a), (b), (c), (d) refer to radiation pattern and in Figure 4.7, where (a), (b), (c), (d) refer to polar plot. As shown in figure the directivity of conventional antenna is 5.17 dBi and 5.41 dBi at 4.66 GHz and 5.61 GHz respectively, while the directivity of RRPs antenna is 5.21 dBi and 5.45 dBi at 4.68 GHz and 5.58 GHz respectively, so the directivity of antenna with inserting RRPs is partially higher than conventional directivity. The beam main lobe direction of conventional antenna is 3 degree with beam width 108.9 degree at 4.66 GHz and 8 degree with beam width 70 degree at 5.61 GHz. The beam main lobe direction of RRPs antenna is 2 degree with beam width 107.8 degree at 4.68 GHz and 9 degree with beam width 67.3 degree at 5.58 GHz. Table 4.1 Shows the characteristics that distinguish between the two antennas.

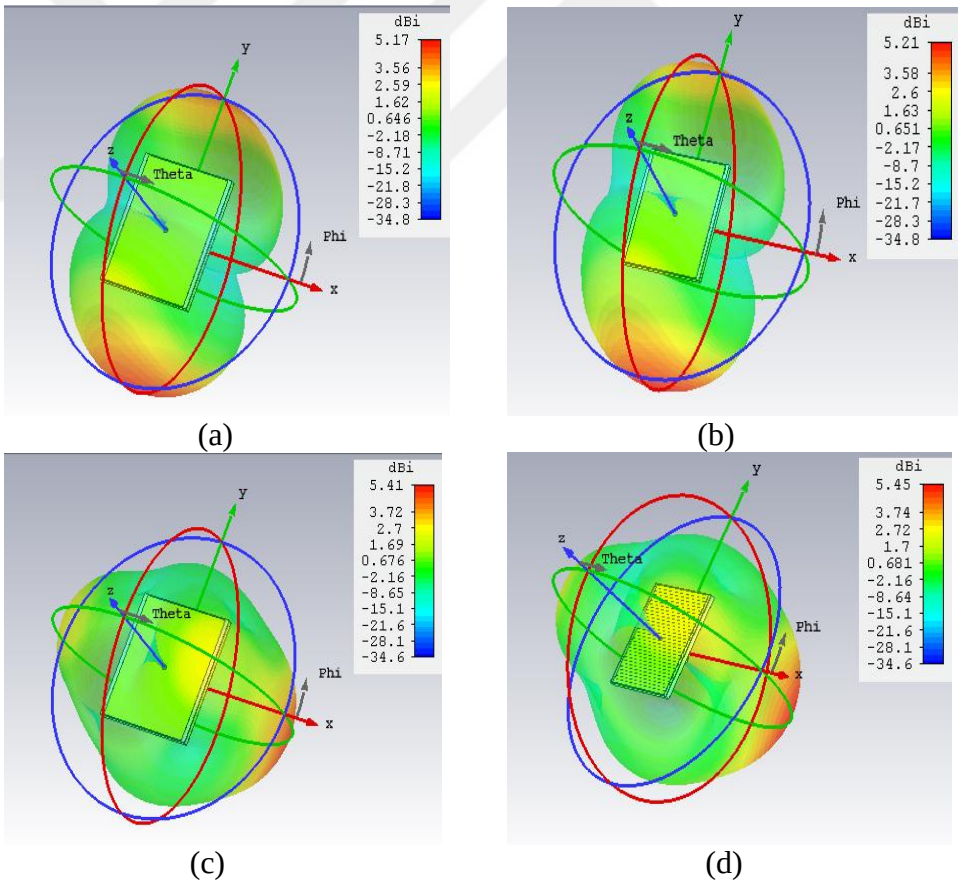

Figure 4.6 Radiation pattern (RP) : a) RP of MSPA at 4.66 GHz, b) RP of RRPs antenna at 4.68 GHz, c) RP of MSPA at 5.61 GHz, d) RP of RRPs antenna at 5.58 GHz

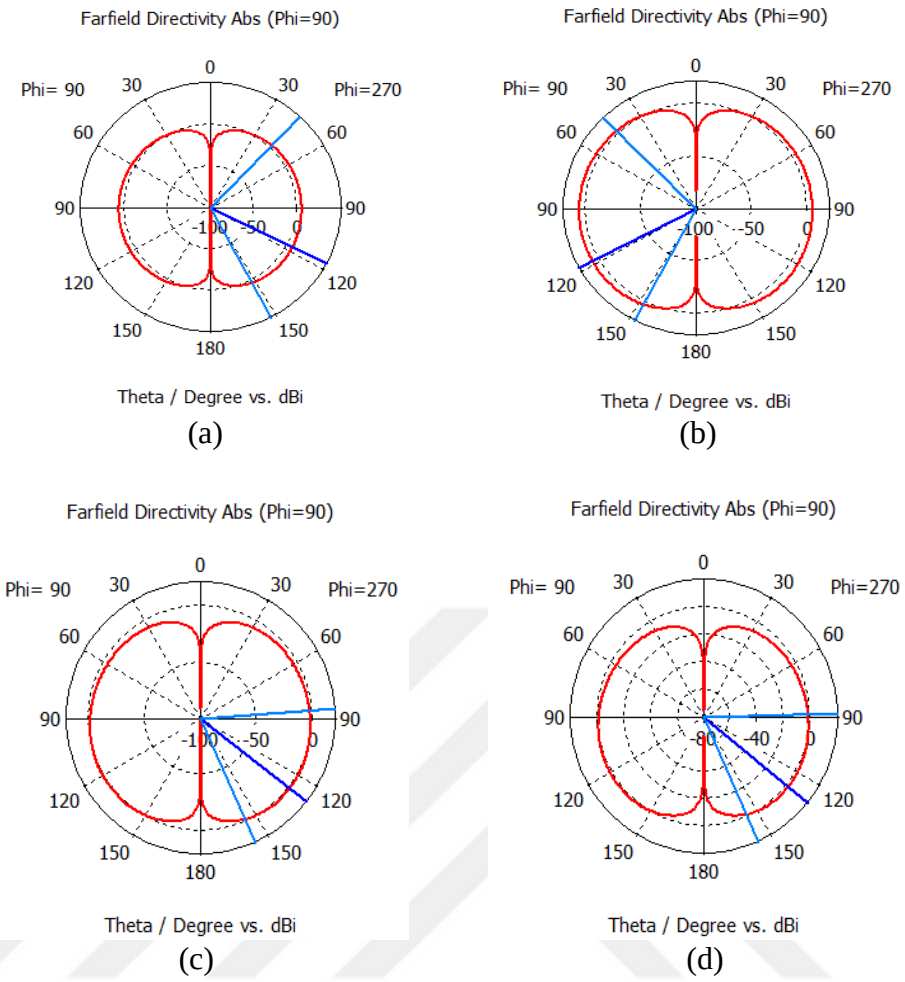

Figure 4.7 Polar plot (PP): a) PP of MSPA at 4.66 GHz, b) PP of RRPs at 4.68 GHz c) PP of MSPA at 5.61 GHz, d) PP of RRPs at 5.58 GHz

Table 4.1 Comparison between conventional and RRPs antennas

Parameter	conventional antenna at 4.66 GHz	RRPs antenna at 4.68 GHz
Return loss dB	-12.7	-14.7
Bandwidth MHz	95	109
Directivity dBi	5.17	5.21
Parameter	conventional antenna at 5.61 GHz	RRPs antenna at 5.58 GHz
Return loss dB	-12.5	-15.4
Bandwidth MHz	114	192
Directivity dBi	5.41	5.45

4.3.2 MSPA with CP Effect

Through simulation results the effect of CP was increasing the return losses, bandwidth, number of bands and minimize the patch size.

4.3.2.1 Return Loss Simulation

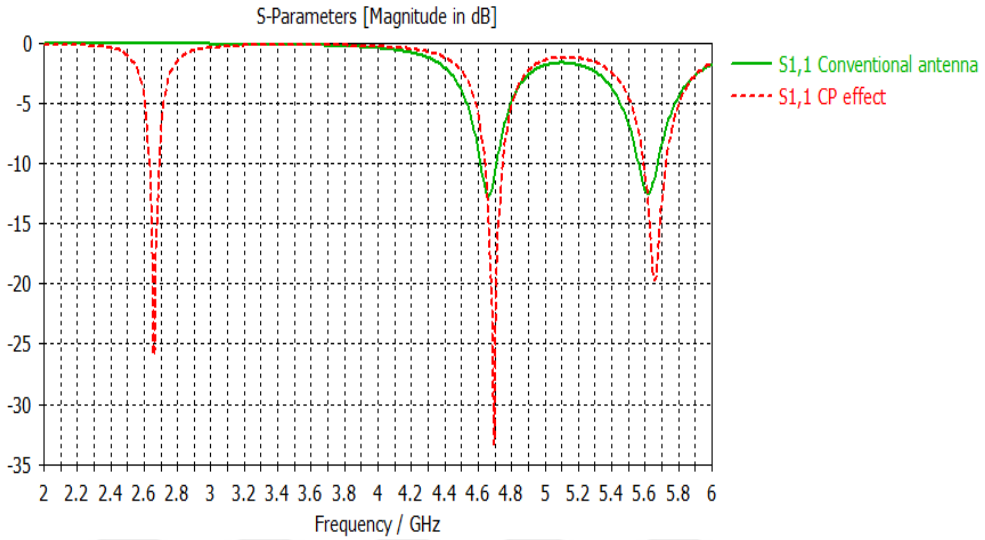

Figure 4.8 Comparison of return losses between MSPA and CP antenna

Figure 4.8 appears the return loss curve S1,1 of the conventional antenna compared to the return loss curve S1,1 of CP. Merging CP with conventional antenna gives better results by increasing the return losses to -25.9dB, -33dB and -19.7dB at 2.65 GHz, 4.69 GHz and 5.65 GHz respectively compared with results of conventional without CP which are -12.7dB and -12.5dB at 4.66 GHz and 5.61 GHz respectively. Note that CP causes slightly shifting in frequencies of MSPA about 30 to 40 MHz and the new created band reduced the size of patch almost by 0.43 and 0.53 respectively. The operating bands of antenna with CP are between 4.640 GHz to 4.746 GHz, 5.590 GHz to 5.725 GHz and 2.631 GHz to 2.688 GHz, so bandwidths of CP-effect antenna are 106 MHz at 4.69 GHz, 135 MHz at 5.65 GHz and 57 MHz at 2.65 GHz compared with conventional antenna which has lower bandwidth about 95 MHz at 4.66 GHz and 114 MHz at 5.61 GHz. so with CP, the bandwidth increases by 11% and 18% respectively plus a new band.

4.3.2.2 Radiation Pattern Simulation

3D radiation pattern and polar plot for both conventional antenna and CP-effect antenna were simulated. The simulating results appear in Figure 4.9, where (a), (b), (c), (d), (e) refer to radiation pattern and in Figure 4.10, where (a), (b), (c), (d), (e) refer to polar plot. As shown in figure the directivity of conventional antenna is 5.17 dBi and 5.41 dBi at 4.66 GHz and 5.61 GHz respectively, while the directivity of CP antenna is 5.31 dBi, 5.26 dBi and 2.23 dBi at 4.69 GHz, 5.65 GHz and 2.65 GHz respectively. Thus, the directivity of antenna with merging CP is slightly greater than conventional directivity at 4.6 GHz and less than directivity of conventional at 5.6 GHz with extra one at 2.65 GHz. The beam main lobe direction of conventional antenna is 3 degree with beam width 108.9 degree at 4.66 GHz and 8 degree with beam width 70 degree at 5.61 GHz. The beam main lobe direction of CP antenna is 2 degree with beam width 109.1 degree at 4.69 GHz, 10 degree with beam width 65.3 degree at 5.65 GHz and 1 degree with beam width 97.6 degree at 2.65 GHz. Table 4.2 Shows the characteristics that distinguish between the two antennas.

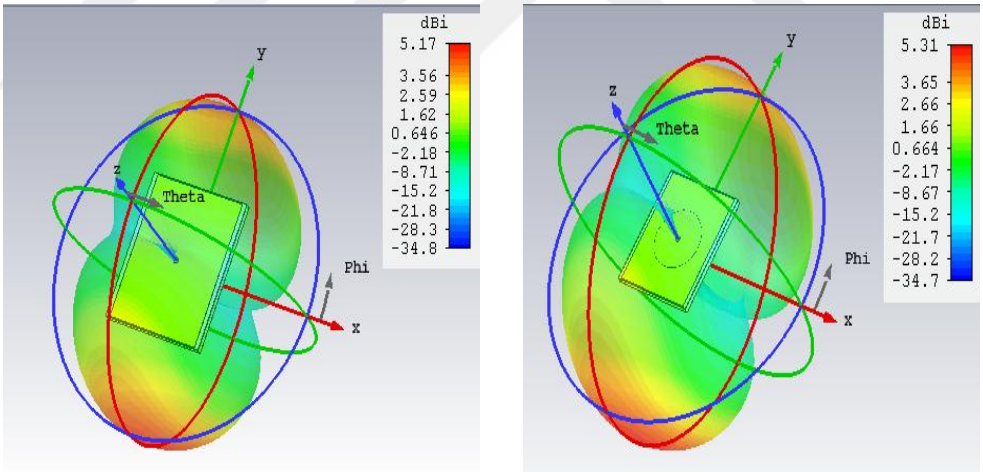

(a) (b)

Figure 4.9 Radiation pattern (RP): a) RP of MSPA at 4.66 GHz, b) RP of CP antenna at 4.69 GHz

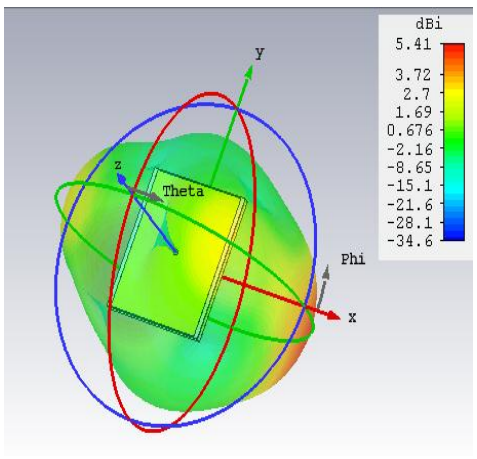

(c)

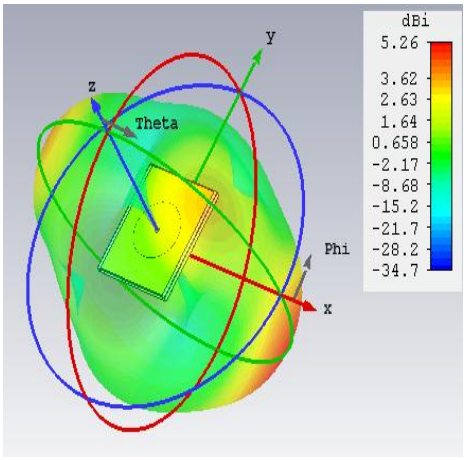

(d)

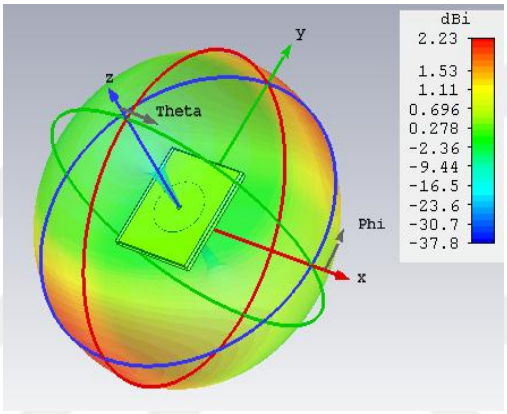

(e)

Figure 4.9 c) RP of MSPA at 5.61 GHz, d) RP of CP antenna at 5.65 GHz, e) RP of CP antenna at 2.65 GHz

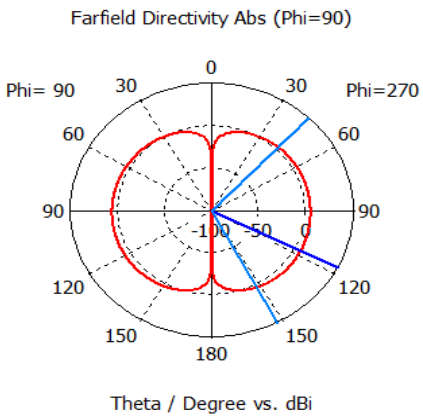

(a)

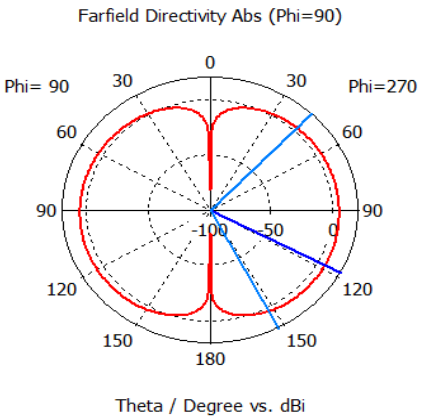

(b)

Figure 4.10 Polar plot (PP): a) PP of MSPA at 4.66 GHz, b) PP of CP at 4.69 GHz

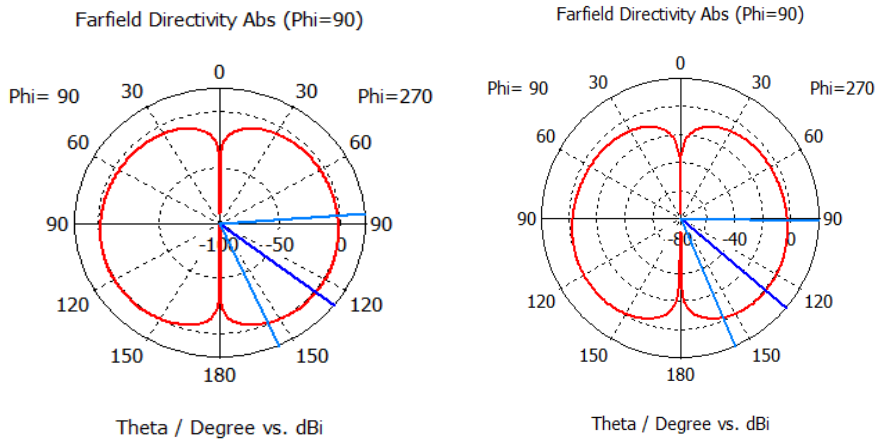

(c)

(d)

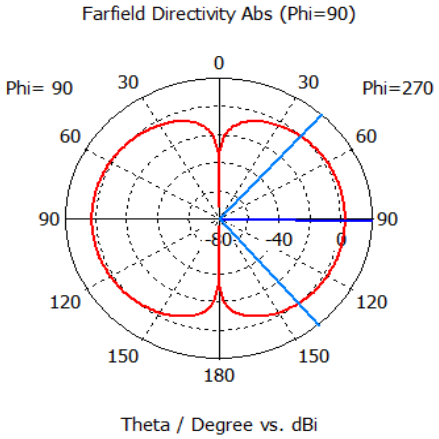

(e)

Figure 4.10 c) PP of MSPA at 5.61 GHz, d) PP of CP at 5.65 GHz, e) PP of CP at 2.65 GHz

Table 4.2 Comparison between conventional and CP antennas

Parameter	Conventional antenna at 4.66 GHz	CP antenna at 4.69 GHz
Return loss dB	-12.7	-33
Bandwidth MHz	95	106
Directivity dBi	5.17	5.31
Parameter	conventional antenna at 5.61 GHz	CP antenna at 5.65 GHz
Return loss dB	-12.5	-19.7
Bandwidth MHz	114	135
Directivity dBi	5.41	5.26

Notice that CP antenna has extra band with parameters -25.9 dB return loss, 57 MHz bandwidth and 2.23 dBi directivity.

4.3.3 MSPA with CRPs Effect

Through simulation results the effect of CRPs was negative on antenna where caused the reduction of return losses and bandwidth. Figure 4.11 shows return loss simulation.

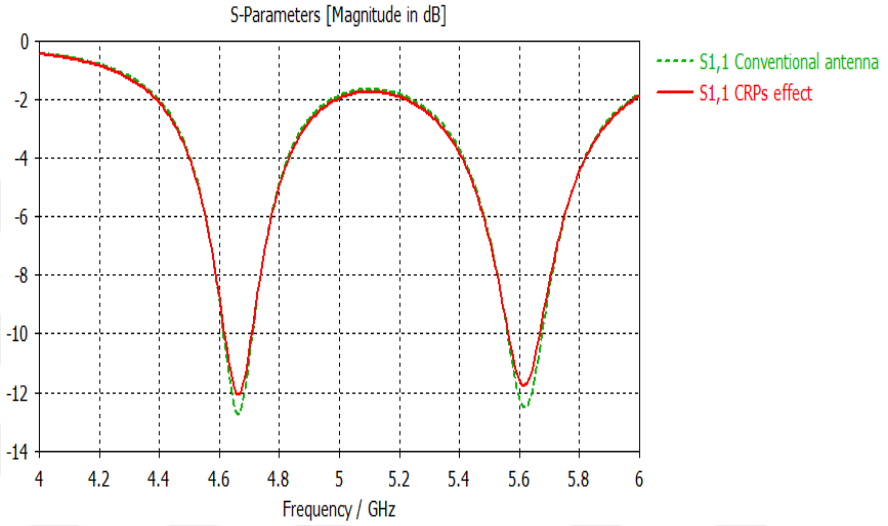

Figure 4.11 Comparison of return losses between MSPA and CRPs antenna

Figure 4.11 appears the return loss curve S1,1 of the conventional antenna compared to the return loss curve S1,1 of CRPs. Adding CRPs to conventional antenna gives bad results by decreasing the return losses to -12dB and -11.7dB at 4.66 GHz and 5.61 GHz respectively, compared with results of conventional. Also CRPs-effect antenna has lower bandwidth than conventional with 89 MHz at 4.66 GHz and 103 MHz at 5.61 GHz. Conclude that the use of CRPs alone with MSPA is negative, later will see its importance when combines with CHDS redirector.

4.3.4 Comparison between the Influential Elements

In this part will see which one of the elements had a greater impact on the antenna. All the parameters clear in Table 4.3.

Table 4.3 Comparison between influential elements

Parameter	RRPs antenna at 4.68 GHz	CP antenna at 4.69 GHz	CRPs antenna at 4.66 GHz
Return loss dB	-14.7	-33	-12
Bandwidth MHz	109	106	89
Directivity dBi	5.21	5.31	5.16
Parameter	RRPs antenna at 5.58 GHz	CP antenna at 5.65 GHz	CRPs antenna at 5.61 GHz
Return loss dB	-15.4	-19.7	-11.7
Bandwidth MHz	192	135	103
Directivity dBi	5.45	5.26	5.34
Parameter	RRPs antenna at 2.65 GHz	CP antenna at 2.65 GHz	CRPs antenna at 2.65 GHz
Return loss dB	-----	-25.9	-----
Bandwidth MHz	-----	57	-----
Directivity dBi	-----	2.23	-----

4.4 MSPA with Metamaterials at 4.66 GHz and 5.61 GHz

This section includes a comparison between the conventional antenna and the metamaterial antennas at 4.66 GHz and 5.61 GHz. The simulation of all were taken to appear the difference in terms of return loss, bandwidth and radiation pattern.

4.4.1 MSPA with CSRR Metamaterial

Through simulation results the action of CSRR in increasing the return losses was evident with slight increase in bandwidth as well as miniaturize the size of patch.

4.4.1.1 Return Loss Simulation

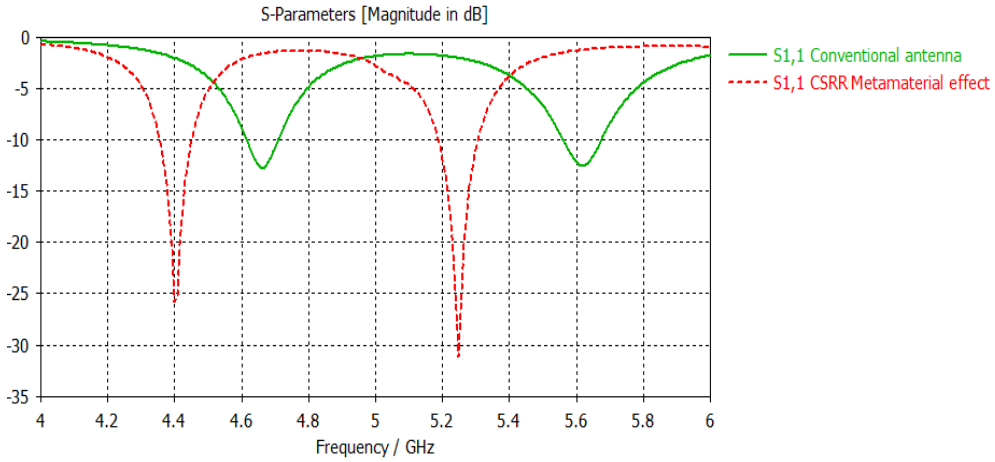

Figure 4.12 Comparison of return losses between conventional and CSRR antennas

Figure 4.12 appears the return loss curve S1,1 of the conventional antenna compared to the return loss curve S1,1 of CSRR. The use of CSRR metamaterial with conventional antenna gives good results by enhancing the return losses to -25.7dB and -31dB at 4.4 GHz and 5.24 GHz respectively, compared with results of conventional without CSRR which are -12.7dB and -12.5dB at 4.66 GHz and 5.61 GHz respectively. Note that CSRR causes a high shifting in frequencies of MSPA about 260 MHz and 370 MHz and that depends on the spacing between rings and area of radiation paths. The shifted band 5.24 GHz gave miniaturization to the patch size about 0.06 and the shifted band 4.4 GHz gave miniaturization about 0.05 and 0.21 respectively. The operating bands of antenna with CSRR are between 4.355 GHz to 4.450 GHz and 5.187 GHz to 5.304 GHz, so bandwidths of CSRR antenna are 95 MHz at 4.4 GHz and 117 MHz at 5.24 GHz compared with conventional antenna which has the same bandwidth of 95 MHz at 4.66 GHz and lower bandwidth of 114 MHz at 5.61 GHz.

4.4.1.2 Radiation Pattern Simulation

3D radiation pattern and polar plot for both conventional antenna and CSRR antenna were simulated . The directivity of conventional antenna is 5.17 dBi and 5.41 dBi at 4.66 GHz and 5.61 GHz respectively, while the directivity of CSRR antenna is 4.97 dBi and 5.08 dBi at 4.4 GHz and 5.24 GHz respectively, so the directivity of antenna with CSRR is partially less than conventional directivity. The beam main lobe direction of conventional antenna is 3 degree with beam width 108.9 degree at 4.66

GHz and 8 degree with beam width 70 degree at 5.61 GHz. The beam main lobe direction of CSRR antenna is 7 degree with beam width 114.3 degree at 4.4 GHz and 7 degree with beam width 74.1 degree at 5.24 GHz. Table 4.4 Shows the characteristics that distinguish between the two antennas.

Table 4.4 Comparison between conventional and CSRR antennas

Parameter	conventional antenna at 4.66 GHz	CSRR antenna at 4.4 GHz
Return loss dB	-12.7	-25.7
Bandwidth MHz	95	95
Directivity dBi	5.17	4.97
Parameter	conventional antenna at 5.61 GHz	CSRR antenna at 5.24 GHz
Return loss dB	-12.5	-31
Bandwidth MHz	114	117
Directivity dBi	5.41	5.08

4.4.2 MSPA with CHDS Metamaterial

This type of CHDS can not be used alone with the antenna because the probe inserted inside the defected CHDS ring without touching the patch, so the role of this structure here as redirector for new frequency selectivity, improved properties and new applications. The probe will be connected to RISs between the substrates and this is what the CHDS will depend on as redirector.

4.5 MSPA with RISs and Metamaterial Structures

In this most important part, the influencing elements will be integrated with the metamaterial structures to configure a complementary antenna. The behavior and impact of the metamaterial will be evident. There will also be comparisons showing the difference between the use of the influencing element and the metamaterial alone and when used together with the antenna.

4.5.1 Conventional Antenna with RRPs and CSRR

The simulation results show that insertion of RRPs with CSRR generated four bands with high return loss, so that gives the antenna a multi-band characteristic as well as miniaturize the patch size.

4.5.1.1 Return Loss Simulation

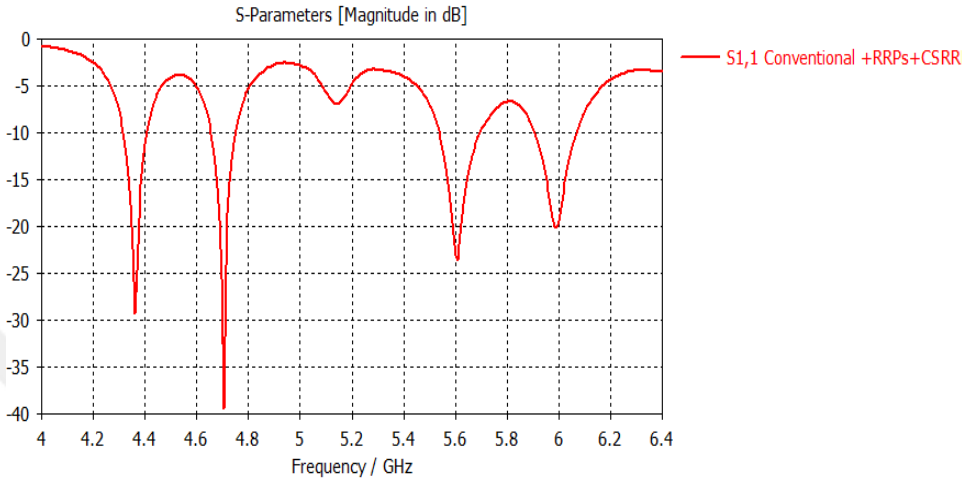

Figure 4.13 Return loss of complementary antenna (MSPA+RRPs+CSRR)

Figure 4.13 appears the return loss curve S1,1 of the integrated antenna which consists of conventional antenna, rectangular ruler patches and complementary split ring resonator. The use of RRPs and CSRR metamaterial together with conventional antenna give better results by increasing the number of bandwidth and enhancing the return loss. Complementary antenna operates at 4.36 GHz, 4.7 GHz, 5.6 GHz and 5.99 GHz with return loss -29.4dB, -39.4dB, -23.6dB and -20dB respectively. The operating bands of antenna are between 4.316 to 4.407 GHz, 4.655 to 4.750 GHz, 5.537 to 5.695 GHz and 5.906 to 6.068 GHz, so bandwidths of antenna are 91 MHz at 4.36 GHz, 95 MHz at 4.7 GHz, 158 MHz at 5.6 GHz and 162 MHz at 5.99 GHz. In the case of this integrated antenna, notice that the two bands of 4.7 GHz and 5.608 GHz have a very low shift about 40 MHz and 8 MHz respectively, compared with conventional which operates at 4.66 GHz and 5.616 GHz. The created new band at 4.36 GHz minimizes the size of the patch by 0.06 and 0.22 respectively. Figure 4.14 shows the return loss simulation of conventional and complementary antennas.

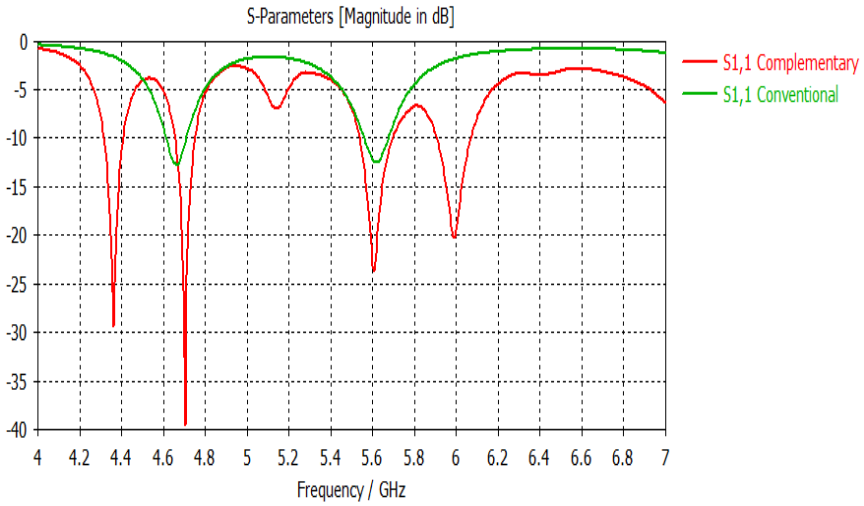

Figure 4.14 Return losses of complementary and conventional antennas

Conclude from Figure 4.14 that the adding of RRPS with CSRR also reduces the shift of bands to other frequencies to make the merged antenna close to matching conventional antenna frequencies with created two extra bands.

4.5.1.2 Radiation Pattern Simulation

3D radiation pattern and polar plot for complementary antenna were simulated. The simulating results appear in Figure 4.15, where (a), (b), (c), (d) refer to radiation pattern and in Figure 4.16, where (a), (b), (c), (d) refer to polar plot. The directivity of antenna is 4.87 dBi, 4.74 dBi, 5.15 dBi and 5.16 dBi at 4.36 GHz, 4.7 GHz, 5.6 GHz and 5.99 GHz respectively. The beam main lobe direction is 6 degree with beam width 112.7 degree at 4.36 GHz, 3 degree with beam width 116.5 degree at 4.7 GHz, 10 degree with beam width 62 degree at 5.6 GHz and 5 degree with beam width 112.8 degree at 5.99 GHz. Table 4.5 shows the characteristics of complementary antenna.

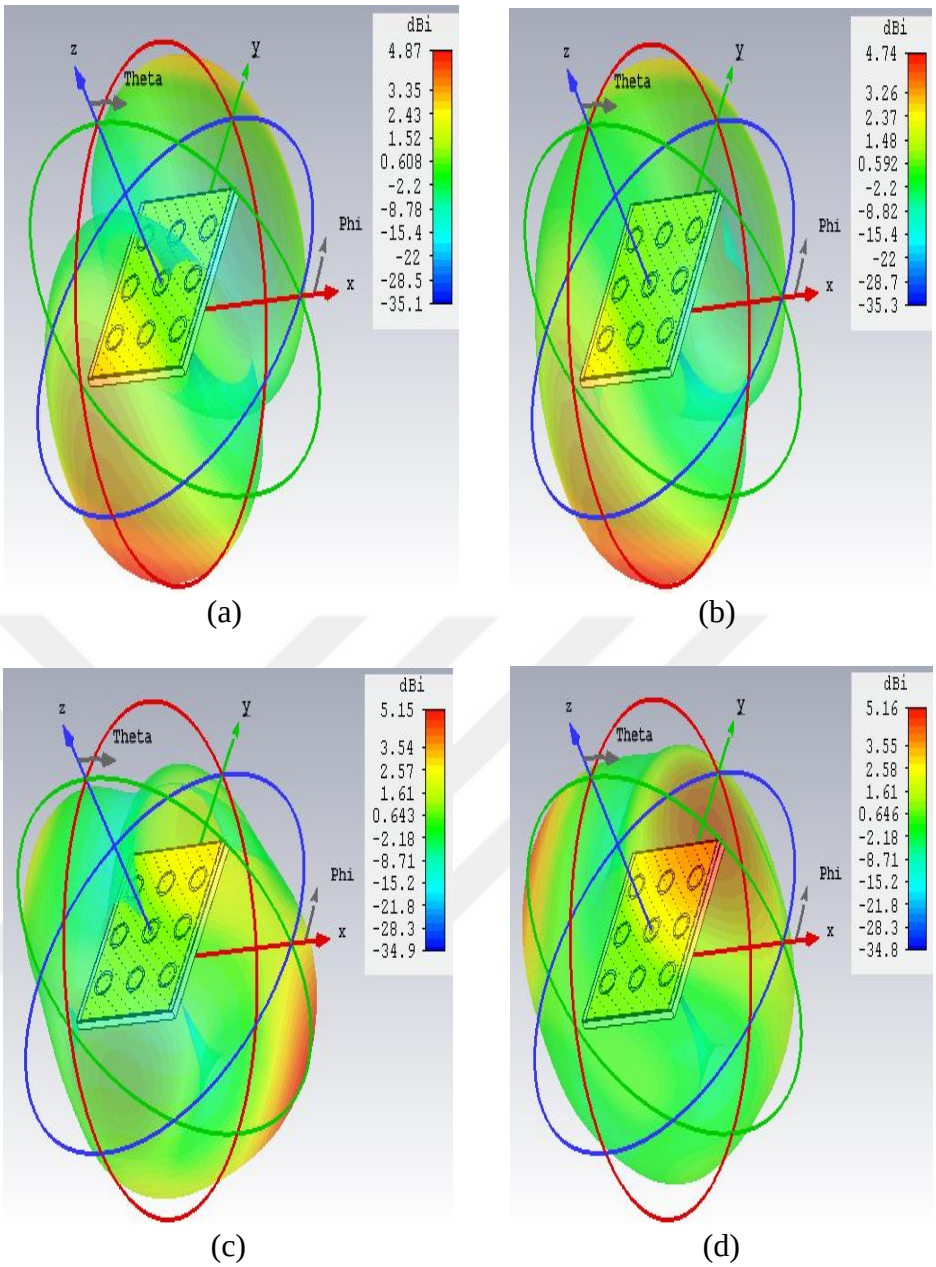

Figure 4.15 Radiation pattern (RP) of complementary antenna: a) RP at 4.36 GHz, b) RP at 4.7 GHz, c) RP at 5.6 GHz, d) RP at 5.99 GHz

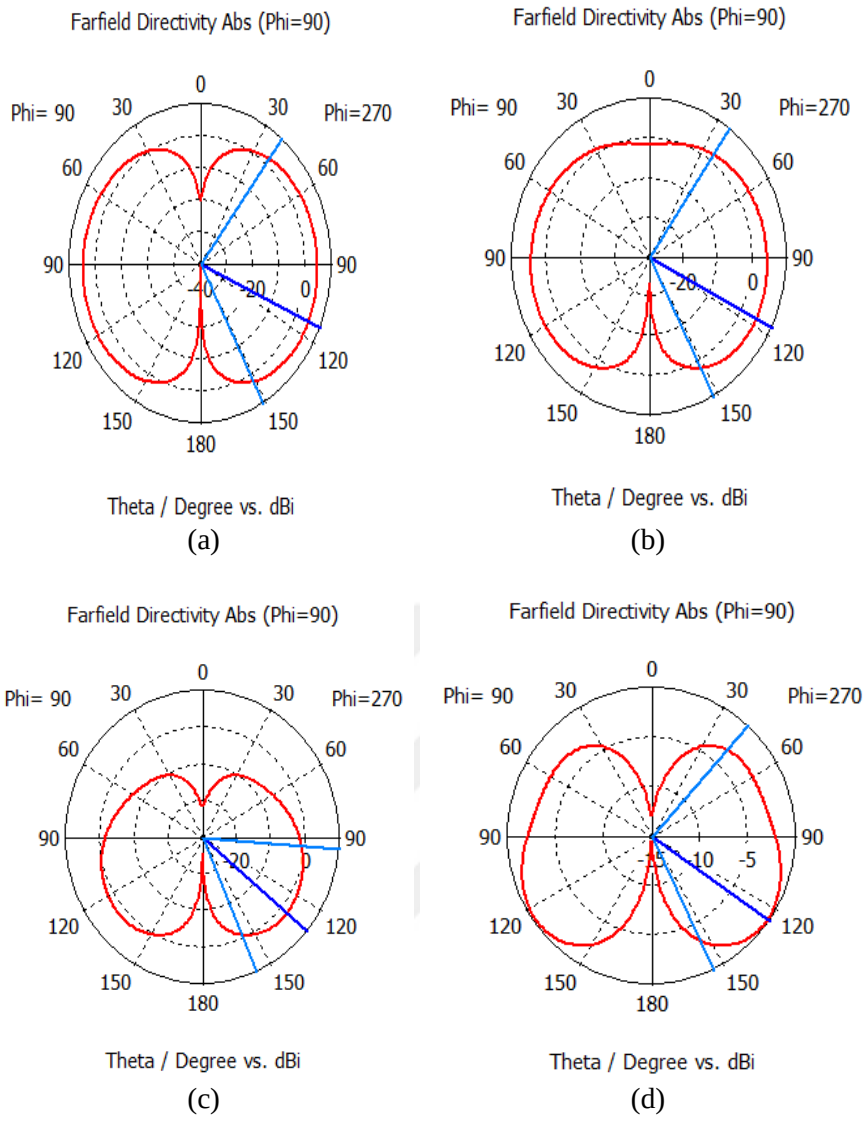

Figure 4.16 Polar plot (PP) of complementary antenna a) PP at 4.36 GHz, b) PP at 4.7 GHz, c) PP at 5.6 GHz, d) PP at 5.99 GHz

Table 4.5 Characteristics of complementary antenna

Parameter	at 4.36 GHz	at 4.7 GHz	at 5.6 GHz	at 5.99 GHz
Return loss dB	-29.4	-39.4	-23.6	-20
Bandwidth MHz	91	95	158	162
Directivity dBi	4.87	4.74	5.15	5.16

4.5.1.3 Change RRPs Dimensions to Minimize the Patch

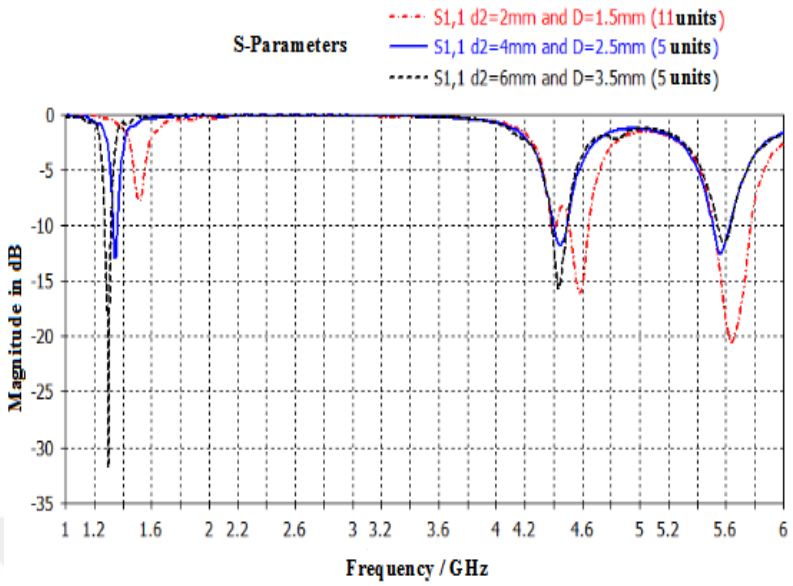

Figure 4.17 Return loss at variable width d2, variable distance between units D and variable number of units.

Figure 4.17 Shows that by increasing the width and distance between RRPs, the return loss of Wi-MAX band will decrease and return loss of GPS band increase. Since, that increase effected on the coupling values between complementary split rings which led to shift the resonant frequencies. The shifted band at 1.3 GHz gave a high miniaturization to the patch size about 0.72 and 0.77 respectively.

4.5.2 Conventional Antenna with CRPs and CHDS

As mentioned previously that the effect of CRPs was negative on antenna but after adding with CHDS which behaves as redirector, the simulation results showed enhancing in return loss and bandwidth with significantly lower patch size.

4.5.2.1 Return Loss Simulation

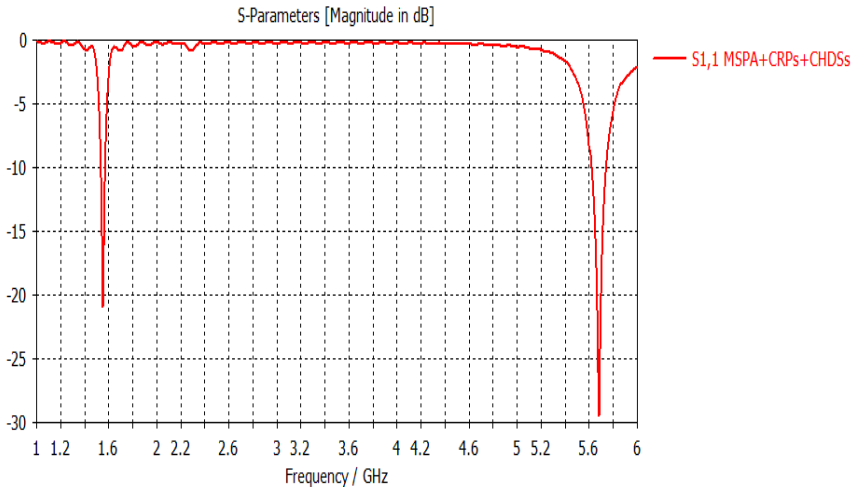

Figure 4.18 Return loss of complementary antenna (MSPA+CRPs+CHDSs)

Figure 4.18 appears the return loss curve S1,1 of the integrated antenna which consists of conventional antenna, circular ring patches and circular head dumbbell structures redirector. The use of CRPs and CHDS metamaterial together with conventional antenna gives better results by enhancing the return loss and bandwidth. Complementary antenna operates at 5.68 GHz and 1.55 GHz with return loss -29.5dB and -20 .95dB respectively. The operating bands of antenna are between 5.616 to 5.739 GHz and 1.534 to 1.570 GHz, so bandwidths of antenna are 123 MHz at 5.68 GHz and 36 MHz at 1.55 GHz. In the case of this integrated antenna, notice that the CHDS caused transition the band of 4.66 GHz to 1.55 GHz as compared with the use of CRPs alone and that gave a high reduction in patch size about 0.67 and 0.72 respectively. Figure 4.19 shows the comparison between CRPs antenna and redirected complementary antenna through the return loss simulation.

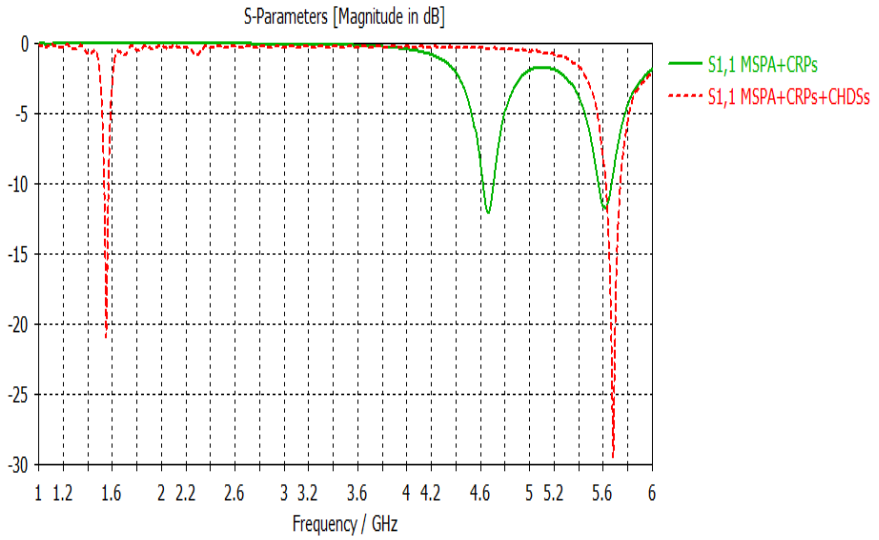

Figure 4.19 Return loss simulation of CRPs and complementary antennas

Figure 4.19 demonstrates the behavior of the CHDS redirector in improvement the return loss and bandwidith of 5.6 GHz and 1.5 GHz to give the antenna special characteristics to work in the applications of WiMAX and GSM, plus large reduction for patch size.

4.5.2.2 Radiation Pattern Simulation

3D radiation pattern and polar plot for complementary antenna were simulated. The simulating results appear in Figure 4.20, where (a), (b) refer to radiation pattern and (c), (d) refer to polar plot. The directivity of antenna is 5.35 dBi and 3.38 dBi at 5.68 GHz and 1.55 GHz respectively. The beam main lobe direction is 7 degree with beam width 68 degree at 5.68 GHz and 3 degree with beam width 107.4 degree at 1.55 GHz. Table 4.6 Shows the characteristics of complementary antenna.

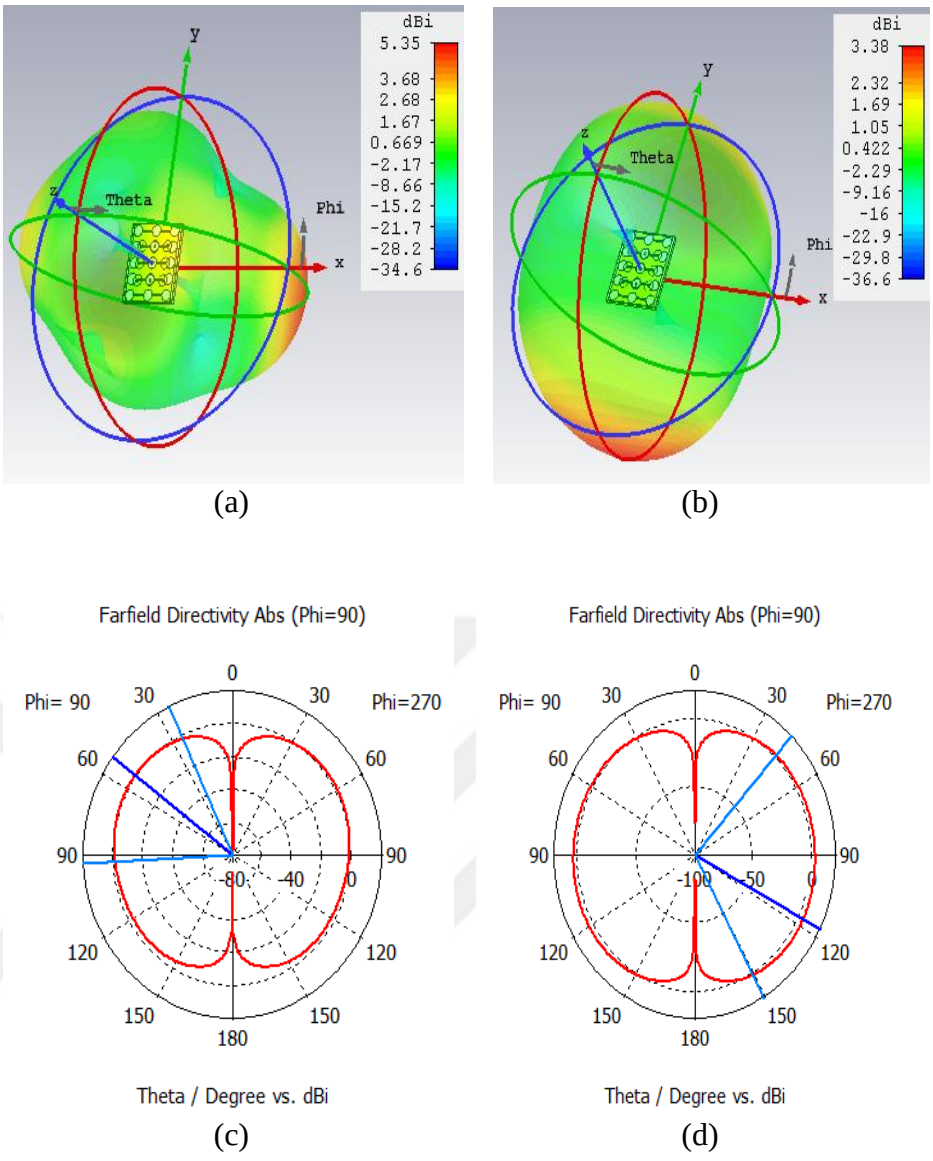

Figure 4.20 Radiation pattern (RP) and polar plot (PP) of complementary antenna: a) RP at 5.68 GHz, b) RP at 1.55 GHz, c) PP at 5.68 GHz, d) PP at 1.55 GHz

Table 4.6 Characteristics of complementary antenna

Parameter	at 5.68 GHz	at 1.55 GHz
Return loss dB	-29.5	-20.95
Bandwidth MHz	123	36
Directivity dBi	5.35	3.38

4.5.3 Study the Behavior of CHDS on CP, CRPs and RRPs

Observed through the simulation results that insertion of circular patch CP, RRPs or CRPs with CHDS shows a dominant and consistent behavior of this structure on antenna. Analysis of this behavior would require many tests with several reactive impedance surfaces RISs that operate at different frequencies. However, the use of CP as a major patch of antenna with CHDS as redirector was very important to understand that behavior because changing the diameter of CP in each case was given a new resonant frequency with the conventional antenna, on the other hand use of RRPs and CRPs also significant to test some different shapes with different dimensions.

4.5.3.1 CP at Diameter (10mm)

As previously mentioned, the return loss of conventional antenna is -12.2dB at 4.66 GHz and -12.1dB at 5.61GHz. Return loss of CP at D=10mm without CHDS is less than conventional just -10.1dB at 5.7 GHz. Adding CHDS increased the return loss to -22dB, also enhanced the bandwidth from 12MHz to132MHz.

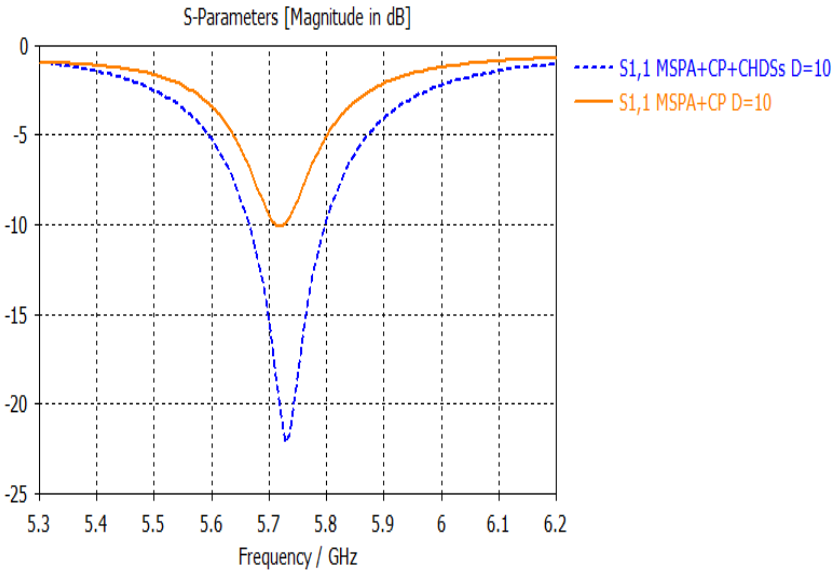

Figure 4.21 Comparison between the CP antenna with diameter of 10 mm and the effect of CHDS behavior

4.5.3.2 CP at Diameter (14mm)

Return loss of CP at D=14mm without CHDS is higher than conventional and has three bands, -22.8 dB at 5.66 GHz, -22.6 dB at 4.7 GHz and -13.8 dB at 3.1 GHz with good bandwidth of 132 MHz, 95 MHz and 62 MHz respectively. Also the created band at 3.1 GHz minimizes the patch by 0.33 and 0.45 respectively. Adding CHDS removed the band of 4.7 GHz and 3.1 GHz with raise in return loss of 5.6 GHz to -35.5 dB and reducing the bandwidth.

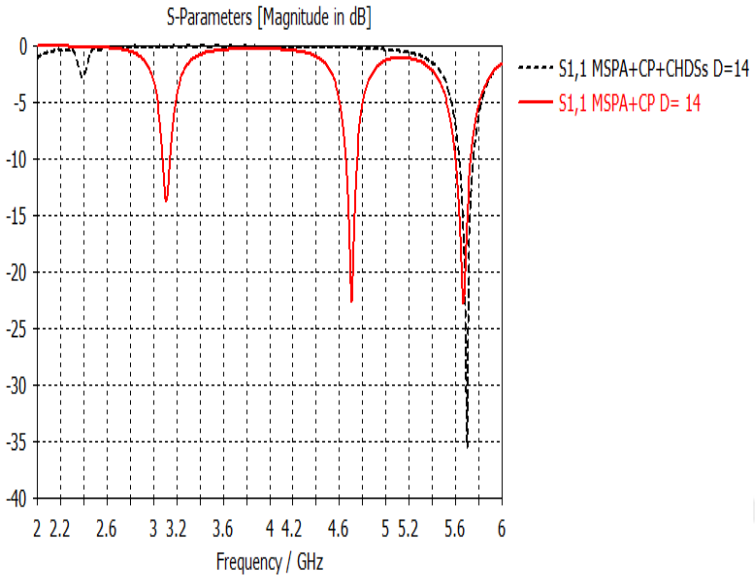

Figure 4.22 Comparison between the CP antenna with diameter of 14mm and the effect of CHDS behavior

4.5.3.3 CP at Diameter (18mm)

Return loss of CP at D=18mm without CHDS has three bands, -18.46dB at 5.65 GHz, -26.5dB at 4.68 GHz and -12.5dB at 2.3 GHz with good bandwidth of 135 MHz, 110 MHz and 32 MHz respectively. The created band at 2.3 GHz minimizes the patch by 0.50 and 0.59 respectively. Adding CHDS removed the band of 4.68 GHz with decrease in return loss of 5.6 GHz to -13.6dB and shift the band of 2.3 GHz to 1.3 GHz with high return loss of -24dB and 37 MHz bandwidth. The shifted band at 1.3 GHz by effect of CHDS gives a high miniaturization to the patch size about 0.72 and 0.77 respectively.

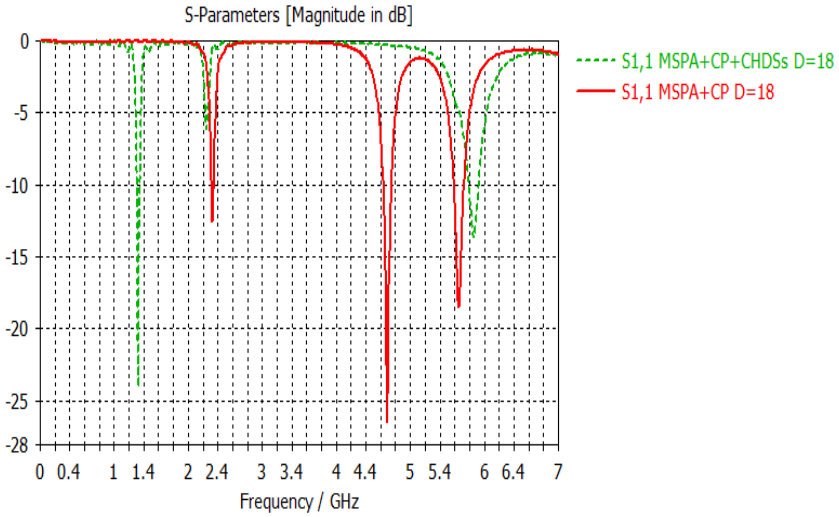

Figure 4.23 Comparison between the CP antenna with diameter of 18mm and the effect of CHDS behavior

4.5.3.4 CHDS with CRPs

Return loss of CRPs without CHDS is less than conventional of -12 dB at 4.66 GHz and -11.7 dB at 5.61 GHz with less bandwidth of 89 MHz and 103 MHz respectively. Adding CHDS improved the return loss and bandwidth to -28.2 dB and 123 MHz at 5.68 GHz and shifted the band of 4.66 GHz to 1.55 GHz with increase in return loss of -20.8 dB and 38 MHz.

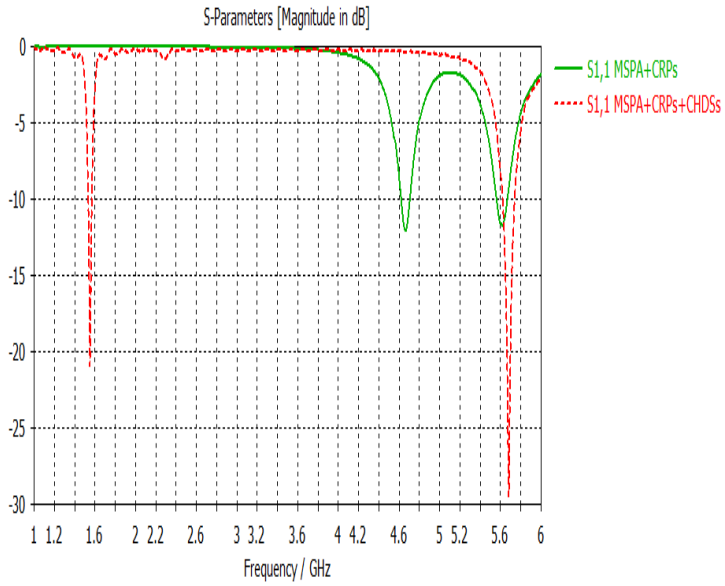

Figure 4.24 Comparison between the CRPs antenna and the effect of CHDS behavior

4.5.3.5 CHDS with RRPs

Return loss of RRPs without CHDS is -14.7 dB at 4.68 GHz and -15.4 dB at 5.58 GHz with bandwidth of 109 MHz and 192 MHz respectively. Adding CHDS reduced the return loss and bandwidth to -11.16 dB and 52 MHz at 5.58 GHz and removed the band of 4.68 GHz.

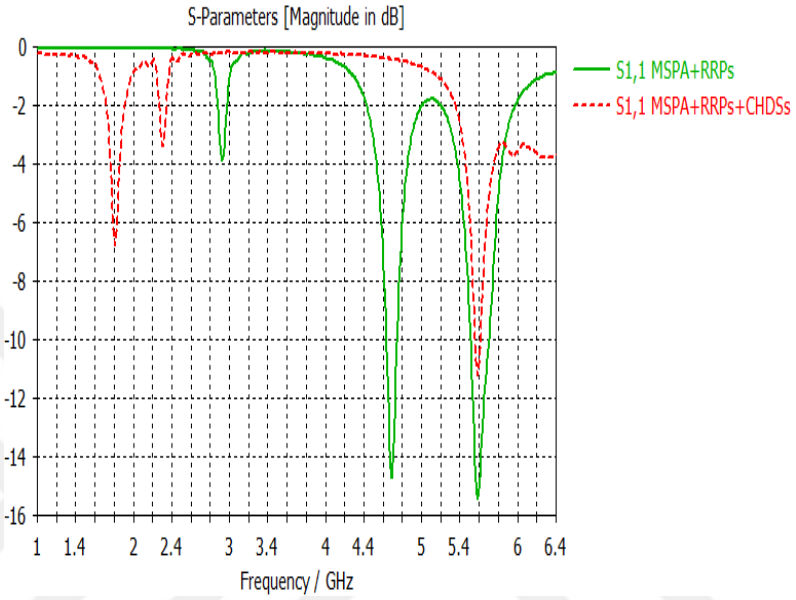

Figure 4.25 Comparison between the RRPs antenna and the effect of CHDS behavior

CHAPTER 5
CONCLUSION

Two types of metamaterials and three types of reactive impedance surfaces were used to enhance the antenna performance:

1. The use of CSRR with RRPs generated quad-band antenna with high return loss and enhanced bandwidth for several applications.
2. The use of CHDS with CRPs antenna generated double-band antenna with improving the return loss and bandwidth for Wi-MAX and GPS applications.
3. The use of CSRR with RRPs, CHDS with CRPs antenna, CHDS with CP antenna and CP alone caused a high reduction in patch size.
4. The CSRR alone caused a slightly miniaturization, while CRPs and RRPs alone did not reduce the patch size.
5. The employment of CSRR alone and CP alone with antenna resulted in an increased return loss at a good rate, while the use of RRPs alone gave low improvement and use CRPs alone had bad effect on return loss.
6. The usage of RRPs alone with antenna provided a high bandwidth and CP has a good B.W, while CSRR has a very small improvement and CRPs has bad effect on bandwidth.
7. The CHDS has the ability to convert the frequencies of conventional antenna to lower frequencies, therefore represents a high quality factor for patch size miniaturization as well as confirmed its importance in Wi-MAX and GPS applications. The changing of CHDS dimensions make it loses its properties.

Investigation and Conclusion of CHDS Behavior

Conclude from that, the CHDS redirector deals with RRPs, CRPs and CP antennas according to the effect of RISs elements on the conventional antenna and depend on the return loss as following:

- If the RIS has a return loss less than -10 dB with negative impact on the conventional antenna by reducing its return loss, the CHDS will increase the return loss and bandwidth of Wi-MAX frequencies which between (5.25-5.85) GHz and shifts (4, 3, 2) GHz frequencies band to the GPS band.
- If the return loss of the RIS is between (-10 dB to -20 dB) and has higher return loss than conventional, the CHDS will reduce the return loss and bandwidth of Wi-MAX frequencies that between (5.25-5.85) GHz and removes (4, 3, 2) GHz frequencies band.
- If the return loss of the RIS is less than -20 dB and higher than conventional, the CHDS will increase the return loss and decreases bandwidth of Wi-MAX frequencies which between (5.25-5.85) GHz and removes (4, 3, 2) GHz frequencies band.

REFERENCES

[1] Stutzman, Warren L., and Gary A. 2012. Thiele. Antenna theory and design. John Wiley & Sons.

[2] Howell, J. (1975). "Microstrip antennas, " IEEE Transactions on Antennas and Propagation, **23**, 90-93.

[3] Deschamps. G. A. (1953). "Microstrip microwave antennas," presented at the Third USAF Symp. on Antennas.

[4] Pozar, D.M. (1992). "Microstrip antennas, " Proceedings of the IEEE, **80**, 79-91.

[5] Huda A. Majid, Mohamad Kamal A. Rahim, and Thelaha Masri. (2008). "Left Handed Metamaterial Design For Microstrip Antenna Application", IEEE International RF And Microwave Conference Proceedings, 2-4.

[6] Mutiara A. B. , Refianti R., and Rachmansyah. (2011). "Design of microstrip patch antenna for wireless communication at 2.4 GHz," Journal of Theoretical and Applied Information Technology, **33**.

[7] Lo, T. K. and Hwang. Y. (1997). "Microstrip antennas of very high Permittivity for personal communications," Asia Pacific Microwave Conference, 253–256.

[8] Sainati, R. A. (1996). CAD of Microstrip Antennas for Wireless Applications, Artech House, Norwood, MA.

[9] Wang, H. Y. and Lancaster. M. J. (1999). "Aperture-coupled thin film superconducting meander antennas," IEEE Transaction on Antennas and Propagation, **47**, 829–836.

[10] Waterhouse, R. (2007). Printed Antennas for Wireless Communications, John Wiley & Sons Inc.

[11] Rajeshkumar V., and Raghavan. S. (2013). "A compact CSRR loaded dual band MPA for wireless applications," IEEE International conference on Computational Intelligence and Computing Research, 1-4.

[12] Issa I. B., and Essaaidi. M. (2013). “Compact Multi-Band Square Complementary SRR Patch Antenna For Wireless Applications,” Mediterranean Microwave Symposium, 1-4.

[13] Bait-Suwailam M. M, and AI-Rizzo. H. M. (2013). “Size Reduction of Microstrip Patch Antennas Using Slotted Complementary Split-Ring Resonators,” International Conference on Technological Advances in Electrical, Electronics and Computer Engineering, 528-531.

[14] Basaran S. C., Olgun U., and Sertel. K. (2013). “Multiband monopole antenna with complementary split-ring resonators for WLAN and WiMAX applications,” Electronics Letters, **49**.

[15] Vakani M. U., Wandra K. H., and Sarvaiya. A. K. (2012). “Comparative Analysis of Small Size Dual Band SRR Based Antenna,” Nirma University International Conference on Engineering, 1-4.

[16] Basaran S. C. (2012). “A compact dual-wideband antenna based on complementary split-ring resonator,” Microwave and Optical Technology Letters, **54**, 1917–1919.

[17] Dong Y., Toyao, H., Itoh, T. (2012). Design and characterization of miniaturized patch antennas loaded with complementary split-ring resonators, IEEE Trans. Antennas Propag., **60**, 772 - 785.

[18] Cao W., Xiang Y., Zhang B., Liu A., Yu T., and Guo. D. (2011). “A Low-Cost Compact Patch Antenna With Beam Steering Based on CSRR-Loaded Ground,” IEEE Antennas and Wireless Propagation Letters, **10**, 1520-1523.

[19] Quevedo-Teruel Ó., Moukehn M. N., and Rajo-Iglesias E. (2011). “Dual-Band Patch Antennas Based on Short-Circuited Split Ring Resonators,” IEEE Transactions on Antennas and Propagation, **59**, 2758-2765.

[20] Ortiz N., Falcone F., and Sorolla. M. (2011). “Radiation Efficiency Improvement of Dual Band Patch Antenna Based on Complementary Rectangular Split Ring Resonators,” Proceedings of 5th European Conference on Antenna and Propagation, 830-834.

[21] Ke L., Guang-Ming W., Tong X., and He-Xiu X. (2010). “A Novel Circularly Polarized Antenna Based on the Single Complementary Split Ring Resonator,” International Symposium on Signals Systems and Electronics, **2**, 1-4.

[22] Jahun, K. I. (2015). “Development of triple band planar inverted-H antenna for DCS, WiMAX and WLAN applications”, master thesis.

[23] Baena J. D., Bonache J., Martin F., Sillero R. M., Falcone F., Lopetegi T., Laso M. A. G., Garcia-Garcia J., Gil I., Portillo M. F. and Sorolla M. (2005). "Equivalent-circuit models for split-ring resonators and complementary split-ring resonators coupled to planar transmission lines," IEEE Trans. Microwave Theory Tech., **53**, 1451-1460.

[24] Marques R., Medina F. And Rafii-El-Idrissi R. (2002)."Role of bianisotropy in negative permeability and left-handed metamaterials," Physical Review B, **65**,144440-1.

[25] Baena J. D., Marques R., Medina F. and Martel J., (2004). "Artificial magnetic metamaterial design by using spiral resonators, " Physical Review B, **69**, 14402-1.

[26] Yi-Jang Hsu and Jyh-Long Chern. (2004). "Transmission characteristics of smiling pattern resonators," *Japanese Journal of Applied Physics, Part 2 (Letters)*, **43**, 669-72.

[27] Yi-Jang Hsu, Yen-Chun Huang, Jiann-Shing Lih and Jyh-Long Chern. (2004). "Electromagnetic resonance in deformed split ring resonators of left-handed metamaterials," *J. Appl. Phys.*, **96**, 1979-82.

[28] Falcone F., Lopetegi T., Laso M. A. G., Baena J. D., Bonache J., Beruete M., Marques R., Martin F., and Sorolla M. (2004). "Babinet Principle Applied to the Design of Metasurfaces and Metamaterials," Phys. Rev. Lett., **93**.

[29] Enge, P.; Misra, P. (1999). "Special Issue on Global Positioning System." Proceedings of the IEEE, **87**, 3-15.

[30] Sarkar D., Srivastava K. V., and Saurav K. (2014). "A compact microstrip-fed triple band-notched ultra-wideband monopole antenna," IEEE Antennas Wireless Propag. Lett., **13**, 396–399.

[31] Wang J., Yin, Y.Z., Xie, J.-J., Pan, S.L., Wang, J.-H, Lei, X. (2011). A compact multiband monopole antenna for WLAN/WiMAX applications, Progress In Electromagnetics Research Letters, **23**, 147-155.

[32] Garg R., Bhartia P., Bahl I., and Ittipiboon A. (2001). Microstrip Antenna Design Handbook. Boston, MA, USA: Artech House.

[33] Marrzudi W.N.W, Abidin Z.Z. (2013). "Dual-wideband G-shaped slotted printed monopole antenna for WLAN and WiMAX applications" IEEE International RF and Microwave Conference (RFM), 225-227.

[34] Khan M.R, Morsy M.M and Harackie F.J. (2011). " Miniaturized multiband planar antea for GSM, UMTS, WLAN and WiMAX bands" IEEE International Symposium Antenna and Propagation, 1387- 1389.

[35] Abu Tarboush H.F, Nasif H, "Multiband and Wideband Monopole Antenna for GSM900 and other Wireless Applications" IEEE Antenna and Wireless Propagation, 536-542.

[36] available at: http://www.rfwireless-world.com/Terminology/WiMAX-vs-WLAN.html, November 22, 2017.

[37] Chen W. L, W. G. M and Zhang C. X. (2009). " Bandwidth enhancement of a microstrip-line fed printed wide-slot antenna with a fractal-shaped slot," IEEE Trans. Antennas Propag., **57**, 2176-2179.

[38] Hwang see C., Abd-Alhameed R. A, and Zhou D. (2010). "A crescent-shaped Multiband planar monopole antenna for mobile wireless applications" IEEE antennas and wireless Propag. Letter, **9**.

[39] Narangi T. and Jain S. (2013)."Microstrip Patch Antenna - A Historical Perspective of the Development," Conference on Advances in Communication and Control Systems.

[40] available at: http://www.electronicdesign.com/communications/back-basics-impedance-matching-part-1, July 24, 2017.

[41] available at: http://emlab.utep.edu/ee5390em21/Lecture%2020%20--%20FSS%20and%20Metasurfaces.pdf, March 4, 2017.

[42] available at: https://www.quora.com/Do-spherical-magnets-attract-each-other-or-repel, Jan 3, 2018.

[43] available at: https://www.google.com.tr/search?q=electromagnetic+field+from+circle&source=lnms&tbm=isch&sa=X&ved=0ahUKEwjZlbOElb7YAhUMDMAKHcAqC_MQ_AUICigB&biw=1280&bih=694#imgrc=lRupP2T334SGVM, December 20, 2017.

[44] AL-Shathr Amer H., Yetkin Golge. 2017. "Design of Multiband Antennas loaded with arrays of CSRR and Circular Head Dumbbell Structure", The International Journal of Energy and Engineering Sciences, **2**, 10-20.